

# 000 001 002 003 004 005 ELLMOB: EVENT-DRIVEN HUMAN MOBILITY GEN- 006 ERATION WITH SELF-ALIGNED LLM FRAMEWORK 007 008 009

010 **Anonymous authors**  
011  
012  
013  
014  
015  
016  
017  
018  
019  
020  
021  
022  
023  
024  
025  
026  
027  
028  
029  
030  
031  
032  
033  
034  
035  
036  
037  
038  
039  
040  
041  
042  
043  
044  
045  
046  
047  
048  
049  
050  
051  
052  
053  
054  
055  
056  
057  
058  
059  
060  
061  
062  
063  
064  
065  
066  
067  
068  
069  
070  
071  
072  
073  
074  
075  
076  
077  
078  
079  
080  
081  
082  
083  
084  
085  
086  
087  
088  
089  
090  
091  
092  
093  
094  
095  
096  
097  
098  
099  
100

Paper under double-blind review

## ABSTRACT

Human mobility generation aims to synthesize plausible trajectory data, which is widely used in urban system research. While Large Language Model-based methods excel at generating routine trajectories, they struggle to capture deviated mobility during large-scale societal events. This limitation stems from two critical gaps: (1) the absence of event-annotated mobility datasets for design and evaluation, and (2) the inability of current frameworks to reconcile competitions between users' habitual patterns and event-imposed constraints when making trajectory decisions. This work addresses these gaps with a twofold contribution. First, we construct the first event-annotated mobility dataset covering three major events: Typhoon Hagibis, COVID-19, and the Tokyo 2021 Olympics. Second, we propose ELLMob, a self-aligned LLM framework that first extracts competing rationales between habitual patterns and event constraints, based on Fuzzy-Trace Theory, and then iteratively aligns them to generate trajectories that are both habitually grounded and event-responsive. Extensive experiments show that ELLMob wins state-of-the-art baselines across all events, demonstrating its effectiveness.

## 1 INTRODUCTION

Human mobility generation aims to synthesize plausible spatio-temporal trajectories of human movement (Kim et al., 2024). The study of such trajectories offers deep insights for urban planning, transportation management, and public health (Duan et al., 2023; Chen et al., 2023; Li et al., 2024). Moreover, synthetic trajectories provide a privacy-preserving alternative that permits broader access and usage than sensitive real-world data. The emergence of Large Language Models (LLMs) has modeled trajectories as a “spatio-temporal language on a map,” shifting the task from data distribution learning of traditional methods to instruction-based text generation (Choi et al., 2020; Feng et al., 2025). They leverage powerful contextual understanding and reasoning capabilities, offering advantages in semantic interpretability and versatility to different scenarios (Wang et al., 2024).

Current LLM-based methods explore various modeling strategies for generating realistic trajectories. One line of work studies single-stage direct prompting. For example, Wang et al. (2023); Feng et al. (2024) concatenate available information such as long and short-term check-ins and instruct an LLM to jointly model user preferences, geospatial distance, and sequential dynamics, yielding coherent trajectories. Profile augmented modeling with a multi-stage pipeline is also a prominent research direction. For instance, Wang et al. (2024); Gong et al. (2024); Ju et al. (2025) first apply an LLM to infer semantic profiles from user histories such as personas and travel motivations, and then condition generation on these high-level abstractions to produce personalized trajectories.

Although these methods achieve remarkable success, they still suffer from two key weaknesses. The first is **data scarcity leading to evaluation bias**. These methods are developed and evaluated primarily on datasets dominated by non-event days (stable period), resulting in questionable reliability when modeling non-routine deviations caused by large-scale societal events (e.g., natural disasters, public-health emergencies) (Zhong et al., 2024). As Figure 1 (a) illustrates, during a typhoon, travel shifts away from coastal areas and unnecessary commutes are eliminated. Without reliable data to evaluate their performance in modeling these dynamics, the reliability of these models for downstream applications, such as emergency response planning and transportation management under stress, is severely reduced (Li et al., 2017). Another limitation is **lack of a mechanism to reconcile competing decisions**. In these events, real-world human mobility combines habitual regularities

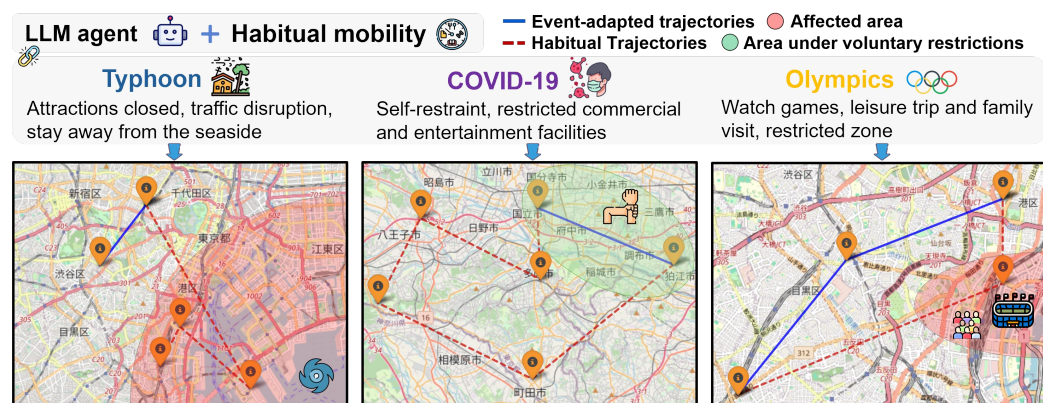


Figure 1: Event-driven mobility generation by LLMs, which incorporates event context to capture real-world human mobility on three different events: (1) Typhoon: evacuation from seaside, (2) COVID-19 Pandemic: self-restraint, and (3) Olympics: restricted zones and traffic jam.

with shock-induced deviation (Song et al., 2014). As Figure 1 (b) and (c) show, while overall mobility patterns are altered, event-adapted trajectories preserve visits to essential anchor points (shared nodes for both lines) of a user’s routine, such as workplaces. Current methods struggle to navigate this duality, producing trajectories that either default to habitual patterns or are dominated by event constraints. Thus, an explicit reconciliation mechanism is needed to generate plausible trajectories.

To tackle these challenges, we first develop an event-centric dataset to provide the necessary empirical foundation for studying non-routine mobility. It covers trajectories from over a thousand users in the Tokyo metropolitan area cross three large-scale societal events (COVID-19 Pandemic, Typhoon Hagibis, Tokyo Olympics) with distinct mobility effects, in addition to a normal period for baseline comparison. **Second, we introduce ELLMob, a self-aligned LLM framework that incorporates cognitive theory to shift generic self-alignment from error correction to conflict reconciliation, explicitly arbitrating between these competing decisions.** Our key insight draws from Fuzzy-Trace Theory (FTT) (Reyna & Brainerd, 1995), which posits that *gist*, the essential meaning distilled from information, guides decisions under uncertainty. Event-driven mobility naturally fits this perspective, as individuals weigh habitual patterns against event-imposed constraints. Crucially, FTT reveals that *gist* can be linguistically expressed, enabling us to analyze the decision basis of LLMs. Building on these insights, ELLMob extracts three forms of *gist* to capture competing decision rationales: *pattern gist* (habitual tendencies) and *event gist* (constraint requirements), along with the *action gist* (LLM’s current trajectory decision). Through iterative alignment of these *gists*, ELLMob transforms trajectory decision into a traceable process where competitions are explicitly identified and reconciled, generating habitually grounded and event-responsive trajectories.

Experiments show that on our event-centric dataset, existing methods often produce trajectories that either default to routine patterns or overfit to event shocks (Figure 4), leading to poor generation quality. In contrast, ELLMob effectively reconciles this duality, achieving the best performance across four widely used metrics and surpasses strongest baselines with an average improvement of **46.9%** across all three events (Table 5). Ablation studies confirm the critical role of *gist*-level reconciliation: incorporating cognitive-based self-alignment improves performance by an average of **69.5%** over non-aligned variants, highlighting its necessity for event-driven mobility modeling. Main contributions of this work are summarized as:

- We construct the first event-centric human mobility dataset with detailed semantic information, providing a foundation for studying the non-routine deviations caused by societal events.
- We provide the first empirical evidence that current LLM-based methods struggle to model human mobility under societal events, revealing a critical research gap.
- **We propose an FTT-inspired framework that constructs decision variables to explicitly reconcile conflicts between habitual patterns and event constraints, enabling traceable decision-making.**
- ELLMob achieves state-of-the-art (SOTA) performance across all evaluated scenarios, demonstrating its effectiveness in generating plausible human mobility behaviors.

108 

## 2 RELATED WORK

109 

### 2.1 HUMAN MOBILITY GENERATION

111 The task of human mobility generation focuses on synthesizing realistic trajectories (Sun et al.,  
 112 2023; Gong et al., 2023). Early deep learning methods applied sequential models like LSTMs and  
 113 attention-based RNNs to predict temporal dependencies and personal preferences (Hochreiter &  
 114 Schmidhuber, 1997; Kulkarni & Garbinato, 2017; Gao et al., 2017; 2018; Wang et al., 2018; Feng  
 115 et al., 2018; Luo et al., 2021). To improve trajectory fidelity, subsequent research shifted to deep  
 116 generative models, including GANs (Choi et al., 2020; Wang et al., 2021; Zhao & Wang, 2023; Jia  
 117 et al., 2024) and, more recently, diffusion models (Zhu et al., 2023b;a; Chu et al., 2024), which  
 118 excel at generating high-resolution location sequences. The emergence of LLMs introduced a new  
 119 approach, re-framing trajectory generation as a sequence generation task conditioned on contextual  
 120 prompts (Xue et al., 2022; Wang et al., 2023; Feng et al., 2024). However, the defined task for all  
 121 these preceding models has been to simulate the routine activity trajectories of users. Their ability  
 122 to generate faithful trajectories under sudden, non-stationary conditions such as disasters or public  
 123 health crises therefore remains unknown, compromising their real-world application. Our work  
 124 addresses this deficiency by defining the task of event-driven human mobility generation.

125 

### 2.2 LLM FOR HUMAN MOBILITY MODELING

126 LLMs are currently applied across a range of human mobility modeling strategies (Wang et al., 2023;  
 127 Feng et al., 2024; Wang et al., 2024; Tang et al., 2024; Zhang et al., 2024; Beneduce et al., 2025).  
 128 For example, Wang et al. (2023) incorporated both long- and short-term dependencies from histori-  
 129 cal mobility data into LLMs to generate the next visiting location. Liang et al. (2024) used an LLM  
 130 with historical mobility Origin-Destination data to generate travel demand during public events at  
 131 the Barclays Center. Wang et al. (2024) integrated diverse user contexts, such as activity patterns,  
 132 motivations, and profiles, into an LLM to generate more interpretable daily trajectories. Existing  
 133 LLM-based methods fail to reconcile competing objectives during events: they either blindly follow  
 134 habitual patterns or event constraints, making them unable to effectively adapt to sharp mobility be-  
 135 havioral changes driven by events (Luo et al., 2024). In contrast, ELLMob is cognitive theory-driven  
 136 and incorporates a self-aligned mechanism that iteratively adjusts generated trajectories, shifting the  
 137 generation goal from maximizing statistical likelihood to cognitive plausibility.

138 

## 3 PROBLEM DEFINITION

139 In this section, we define the terminology and formulate the event-driven trajectory genera-  
 140 tion problem. A **trajectory**  $\tau$  is a time-ordered sequence of visited places, represented as  
 141  $\{(p_0, t_0), (p_1, t_1), \dots, (p_n, t_n)\}$ , where each tuple  $(p_i, t_i)$  denotes a visit to place  $p_i$  at time  $t_i$ . **Event**  
 142 **Context**, denoted  $E_{ctx}$ , is structured data describing the exogenous shock associated with a specific  
 143 event  $c$ . For a user  $u$ , we partition their historical trajectories within a pre-event window  $W^{Pre}(c)$   
 144 into two disjoint sets based on a short-term duration  $T_{short-term}$  relative to the start time of event  
 145  $t_c$ : **long-term trajectories**  $D_{long-term}^{(u)} = \{\tau^{(u,d)} \mid d < t_c - T_{short-term}\}$  and **short-term trajectories**  
 146  $D_{short-term}^{(u)} = \{\tau^{(u,d)} \mid d \geq t_c - T_{short-term}\}$ . These two datasets jointly characterize the prior mo-  
 147 bility patterns of the user. The objective of this task is to develop a generative model that generates  
 148 the event-driven trajectory:  $F : (D_{long-term}^{(u)}, D_{short-term}^{(u)}, E_{ctx}) \mapsto \tau$ .

149 

## 4 EVENT HUMAN MOBILITY DATA

150 To develop and evaluate the performance of models in capturing mobility shifts under varying events,  
 151 we construct a dataset from Tokyo trajectories collected via Twitter and Foursquare APIs (2019-  
 152 2021). It encompasses three distinct events selected to represent a spectrum of societal conditions,  
 153 as well as a normal period to establish a baseline. Detailed specifications are provided in Table 1.

154 For prolonged events (COVID-19 Pandemic and Tokyo Olympics), we focus on the first seven days  
 155 to capture pronounced behavioral shifts. COVID-19 Pandemic began with the State of Emergency  
 156 of Japan. 30-day window for normal period is used to establish a robust baseline of typical mo-  
 157 bility, averaging out weekly fluctuations. Pre-event period (two months) acts as training data for  
 158 deep learning baselines and a source for user pattern extraction for LLM-based baselines. Follow-  
 159 ing collection process described in Appendix B, we curated a dataset of 1,100 users who exhibited  
 160 consistently dense check-in activity throughout the study period. Each sample includes user ID, geo-  
 161 graphical coordinates, subcategory, subcategory ID, category, timestamp, and a comment, as shown

162  
163  
164 Table 1: Specifications for experimental evaluation scenarios.  
165  
166  
167  
168

Event	Event Period	Pre-Event Period	Description
Typhoon Hagibis	2019-10-12 ~ 10-13	2019-08-13 ~ 10-11	Natural disaster.
COVID-19 Pandemic	2020-04-07 ~ 04-13	2020-02-07 ~ 04-06	Public health emergency.
Tokyo 2021 Olympics	2021-07-23 ~ 07-29	2021-05-24 ~ 07-22	Pandemic-era large event.
Normal Period	2019-09-01 ~ 09-30	2019-07-03 ~ 08-31	Regular urban mobility.

169  
170 in Appendix C. Table 2 shows key statistics of this dataset. Table 3 compares data dimensions across  
171 major mobility datasets (GeoLife (Zheng et al., 2009), Gowalla (Cho et al., 2011), Foursquare (Yang  
172 et al., 2015), and Yelp (Asghar, 2016)), revealing that ours cover all standard mobility dimensions.  
173 To the best of our knowledge, our dataset is the first to cover a broad spectrum of distinct event  
174 types (long-term vs. short-term, diverse semantics) with continuous, dense pre- and during-event  
175 trajectories, enabling the precise analysis of behavioral transitions during societal shifts.  
176

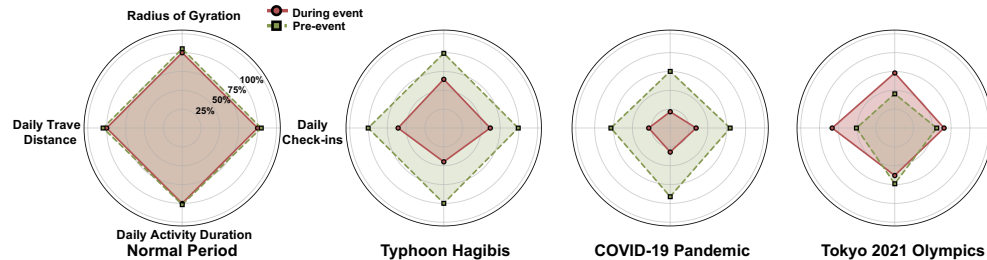
177 Table 2: Dataset statistics by scenario, detailing  
178 the counts of check-ins, unique POIs, and POI  
179 categories, with per-scenario totals.  
180

Event	Check-ins	POIs	Subcat.
Typhoon Hagibis	4,330	2,768	333
COVID-19 Pandemic	8,444	3,887	330
Tokyo 2021 Olympics	16,071	8,103	466
Normal Period	104,792	30,635	654
Agg. Pre-Event	643,027	90,832	763

181 Table 3: T, L, C, TC, N, and E denote time, lo-  
182 cation, subcategory, comments, normal period  
183 and explicit event annotation, respectively.  
184

Dataset	T	L (lat,lon)	C	TC	N	E
GeoLife	✓	✓	✗	✗	✓	✗
Gowalla	✓	✓	✗	✗	✓	✗
Foursquare	✓	✓	✓	✗	✓	✗
Yelp	✓	✓	✓	✓	✓	✗
<b>Ours</b>	✓	✓	✓	✓	✓	✓

185 To quantitatively ground this study, we present a statistical analysis to reveal distinct impacts of each  
186 event on collective mobility. We adopt four widely-used metrics from the human mobility work  
187 (Pappalardo et al., 2015; Alessandretti et al., 2020): daily check-ins, capturing activity intensity, the  
188 radius of gyration and total travel distance, measuring spatial extent and volume, respectively, and  
189 the daily activity duration, quantifying the temporal span. Results are shown in Figure 2. Specifi-  
190 cally, COVID-19 Pandemic and Typhoon Hagibis significantly suppressed the scope and frequency  
191 of movement. In contrast, Olympics reversed suppressive trend in activity of COVID-19 Pandemic.  
192

204 Figure 2: Normalized radar charts of four mobility metrics on pre-event and during-event patterns.  
205206  
207 

## 5 METHODOLOGY

208  
209 

### 5.1 EVENT SCHEMA CONSTRUCTION

210 A challenge in event-driven mobility generation is that real-world events are typically described in  
211 lengthy, free-form text (e.g., news reports and policy documents), which often leads the LLM to  
212 overlook critical information during trajectory generation (Liu et al., 2024; An et al., 2024). To  
213 address this, an event schema construction step is introduced to transform raw event narratives into a  
214 structured representation that explicitly outlines the event’s impact on population mobility patterns.  
215 The event schema is designed around four distinct but complementary aspects that collectively cover  
216 the key information required to assess mobility changes:

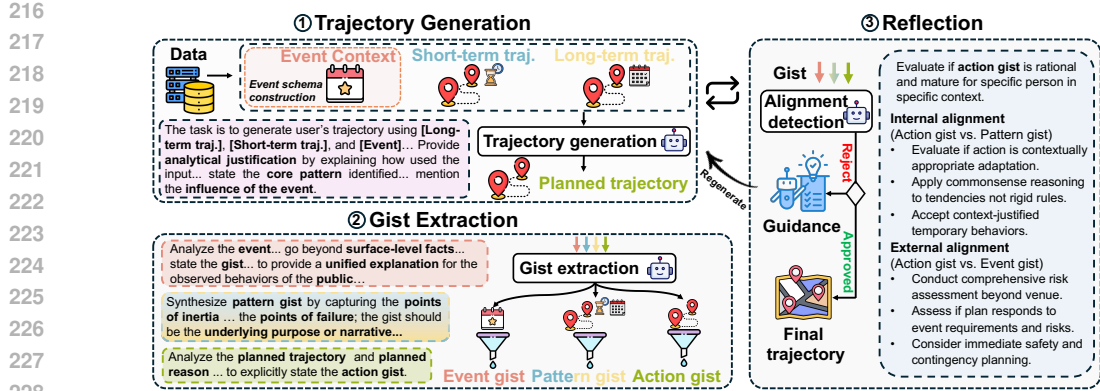


Figure 3: The ELLMob framework architecture comprising three interconnected modules: Trajectory Generation, Gist Extraction, and Reflection-based alignment.

- *Event profile*: Records the fundamental elements of the event (e.g., type, name, occurrence time, and affected regions). This provides an anchor for spatio-temporal alignment.
- *Intensity and scale*: Quantifies key metrics of the event’s severity, such as wind speed and amount of precipitation, to inform travel risk assessment.
- *Infrastructure and service impact*: Describes the operational status of critical resources (e.g., transportation, public venues), defining the physical constraints on mobility.
- *Official directives*: Captures governmental orders and recommendations (e.g., a request for residents to avoid non-essential travel), including their applicable populations and geographic scope, ensuring generated trajectories refer to policy mandates.

An LLM is leveraged to process the raw event text  $E_c$  into a structured key-value format, referred to as event context  $E_{ctx}$ , which subsequently serves as the input to the trajectory generation task. The prompt is provided in [Figure A6](#) and the generated contents are presented in [Appendix E](#).

## 5.2 SELF-ALIGNED LLM FRAMEWORK

In [Figure 3](#), we propose ELLMob, a cognitive theory-driven framework that employs an iterative refinement process to reconcile competition between a user’s habitual patterns and event constraints.

### 5.2.1 THEORY OF PLANNED MOBILITY BEHAVIOR

Fuzzy-Trace Theory (FTT) ([Reyna & Brainerd, 1995](#)) provides a cognitive perspective on decision-making under uncertainty, emphasizing that decisions are driven by *gist*, which refers to the bottom-line (essential) meaning of information rather than *verbatim* details. A classic example is evacuation, where the action is driven not by the exact probability that a tsunami will strike (e.g., 15%) but by the gist that the risk is “high.” According to FTT, gist can be linguistically expressed, making the decision-making basis transparent. In event-driven mobility generation, uncertain disruptions such as natural disasters or epidemics require the model to navigate between two independent decision bases: adhering to habitual mobility routines or complying with event-imposed constraints. Existing LLM-based methods lack an explicit mechanism for arbitrating between these competing decisions, leaving their rationale difficult to audit or control and tending to follow only one gist. By extracting the gist underlying these decisions, we expose the model’s decision basis and resolve competition in a transparent manner. We extract relevant gists: *Pattern Gist* and *Event Gist*, corresponding to two independent decision bases, and *Action Gist*, representing LLM’s tentative plan.

- *Pattern gist*: A representation of the essential tendencies distilled from the user’s habitual mobility patterns, reflecting stable movement routines.
- *Event gist*: A representation of the essential tendencies distilled from contextual constraints, capturing constraints or incentives imposed by external events.
- *Action gist*: A representation of LLM’s immature mobility decision, extracted from the candidate trajectory during planning.

We heuristically formalize these concepts as structured representations, where each gist is derived by assessing the relevant source data along a set of core attributes, which is illustrated in [Table 4](#).

Building on this, we propose a reflection module in which the LLM audits the alignment of these gist. This alignment process explicitly identifies conflicts that are then resolved through guided refinement to ensure that the final generated trajectory is grounded in a unified decision basis. Notably, FTT offers a architecture design basis. It motivates a multi-gist decision framework, guides mapping heterogeneous inputs into a unified gist space for consistent alignment, and drives the use of interpretable bottom-line attributes over arbitrary features. Ablation study is provided in Appendix F.

Table 4: A set of defined core attributes that guide the gist extraction from source information.

Gist Type	Attribute	Description	Example
Pattern Gist	Core Behavior	The dominant pattern of action.	Daily commute to a office.
	Points of Inertia	Deeply embedded, non-negotiable components.	Returning home to a specific neighborhood at night.
	Points of Fracture	Critical dependencies and single points of failure.	Reliance on a single train line that might be suspended.
Event Gist	Primary Intent	Core implication of the event for mobility decisions.	High risk outdoors, strong incentive to stay home.
	Behavioral Implications	Survival, social dynamics, and compliance.	Evacuation from coastal areas, seeking indoor shelter.
	Risk-Reward Calculus	A cost-benefit analysis of the response to event risks.	Risk of injury outweighs reward of a non-essential outing.
Action Gist	Primary Intent	Main purpose driving this trajectory choice.	To get essential supplies from a nearby store.
	Habit Adherence	Degree of preservation in habitual patterns.	Low; this trip deviates from the usual work commute.
	Event Compliance	Trajectory's level of adherence to event constraints.	High; the trip is short and avoids dangerous areas.

### 5.2.2 REFLECTION-BASED ALIGNMENT

We replace single-pass decoding with an iterative reflect-refine loop that externalizes the model’s decision basis for transparent reasoning. Moreover, unlike generic self-alignment approaches that primarily correct errors such as hallucinations, our mechanism targets the decision-making dilemma inherent in event-driven mobility scenarios. Our alignment performs in two stages:

**Alignment Auditing.** This process is dedicated to rigorously auditing the plausibility of a planned trajectory. Each candidate trajectory is checked along two binary dimensions: *Internal alignment* is to ascertain whether the planned trajectory reflects a coherent expression of the user’s intrinsic habitual mobility patterns and current behavioral tendencies. *External alignment* determines if the planned trajectory represents a rational and compliant response to the constraints and implications of the event. A trajectory is accepted only if both criteria are satisfied. The auditor outputs two binary judgments, accompanied by concise rationales that indicate any violated criterion and its cause.

**Corrective Refinement.** Should a planned trajectory fail to satisfy the criteria of either the internal or external alignment audit, ELLMob initiates a corrective refinement loop. During this loop, the precise reasons for the audit failure are provided as feedback to the trajectory generator, guiding it to regenerate a revised trajectory that explicitly addresses the identified semantic misalignments and logical flaws. This loop repeats up to a maximum of  $K$  iterations. A trajectory that satisfies both criteria within the  $K$ -step budget is accepted as a final trajectory. In the rare event that constraints remain unmet after  $K$  iterations, the system executes a fallback strategy. It accepts the last planned trajectory as a best-effort result and explicitly reports the unmet constraints to ensure transparency.

To clearly understand the ELLMob, we show the overall procedure in pseudo-code form Appendix G with complete contents of all related prompts provided in Appendix M.

## 6 EXPERIMENTS

### 6.1 EXPERIMENTAL SETUP

**Baselines.** ELLMob is evaluated against two types of baselines: 1) *deep learning-based methods* which include predictive models: LSTM (Hochreiter & Schmidhuber, 1997), DeepMove (Feng et al., 2018), GETNext (Yang et al., 2022), and MHSA (Hong et al., 2023); and generative models: TrajGAIL (Choi et al., 2020) and DiffTraj (Zhu et al., 2023b). 2) *LLM-based models*: LLM-MOB (Wang et al., 2023), LLM-Move (Feng et al., 2024), LLMOB (Wang et al., 2024), LLM-ZS (Beneduce et al., 2025). For fairness, the input event information remains consistent across all LLM-based

324  
 325 Table 5: Comparison of different methods under three events. Performance is evaluated by JSD  
 326 across four dimensions with the best performance highlighted in **bold**.  
 327

Models	Typhoon Hagibis				COVID-19 Pandemic				Tokyo 2021 Olympics			
	SI↓	SD↓	CD↓	SGD↓	SI↓	SD↓	CD↓	SGD↓	SI↓	SD↓	CD↓	SGD↓
LSTM	0.1336	0.1039	0.0555	0.1111	0.1928	0.1047	0.1300	0.2571	0.1147	0.0651	0.0598	0.0634
DeepMove	0.1697	0.0826	0.0266	0.0759	0.1838	0.0834	0.0423	0.1688	0.1667	0.0492	0.0587	0.0555
GETNext	0.3031	0.2007	0.0274	0.1037	0.2891	0.2241	0.0142	0.1354	0.2701	0.1473	0.0176	0.1204
MHSA	0.1430	0.1815	0.0118	0.0711	0.2180	0.3083	0.0254	0.0437	0.1815	0.2013	0.0120	0.0525
TrajGAIL	0.1034	0.3591	0.0155	0.0275	0.1600	0.3557	0.0195	0.0444	0.0863	0.2913	0.0121	0.0104
DiffTraj	0.1271	0.2450	0.0385	0.0761	0.1405	0.2766	0.0554	0.0454	0.0732	0.2171	0.0342	0.0282
LLMOB	0.0949	0.1195	0.0123	0.0256	0.1013	0.1051	0.0186	0.0286	0.0973	0.0274	0.0110	0.0051
LLM-MOB	0.1214	0.0468	0.0285	0.0344	0.1166	0.0532	0.0234	0.0353	0.1047	0.0286	0.0085	0.0052
LLM-Move	0.1267	0.0392	0.0136	0.0303	0.1408	0.0567	0.0127	0.0503	0.1967	0.0298	0.0101	0.0057
LLM-ZS	0.1574	0.1348	0.0153	0.0724	0.1146	0.0576	0.0552	0.0570	0.0938	0.0330	0.0132	0.0052
ELLMob	<b>0.0642</b>	<b>0.0200</b>	<b>0.0041</b>	<b>0.0173</b>	<b>0.1003</b>	<b>0.0444</b>	<b>0.0080</b>	<b>0.0268</b>	<b>0.0617</b>	<b>0.0061</b>	<b>0.0022</b>	<b>0.0035</b>
w/o I.A.&E.A.	0.1304	0.1270	0.0139	0.0723	0.2331	0.1077	0.1190	0.0733	0.1465	0.0340	0.0093	0.0095
w/o I.A.	0.0835	0.0720	0.0135	0.0436	0.1235	0.0950	0.1053	0.0300	0.1355	0.0316	0.0088	0.0086
w/o E.A.	0.0680	0.0258	0.0077	0.0229	0.2237	0.0860	0.0283	0.0430	0.1392	0.0291	0.0083	0.0064
w/o Eve. Ext.	0.0736	0.0273	0.0045	0.0227	0.2037	0.0741	0.0269	0.0405	0.0686	0.0213	0.0030	0.0041

342  
 343 methods. Specifically, detailed event descriptions (including type, time, location, and constraints)  
 344 are integrated as natural language context at the beginning of each prompt, ensuring that all baselines  
 345 have equal access to the event information despite differences in their specific prompt designs.  
 346

347 **Evaluation Metrics.** *Step Interval (SI).* The time between consecutive activities, defined as  
 348  $SI_t = \tau_{t+1} - \tau_t$ , where  $\tau_t$  denotes the timestamp at step  $t$ ; *Step Distance (SD)*. The distance between  
 349 consecutive locations, defined as  $SD_t = \|l_{t+1} - l_t\|_2$ , where  $l_t \in \mathbb{R}^2$  denotes the location at step  
 350  $t$ . *Category Distribution (CD)*. This metric captures the distribution of activity types. To calculate  
 351 it, we aggregate the total number of visits  $N(c_k)$  for each location category  $c_k$ . *Spatial Grid Dis-*  
 352 *tribution (SGD)*. It captures the population-level spatial footprint of activities. All visited locations  
 353 are discretized onto a fixed  $S \times S$  grid covering the Tokyo metropolitan area, with visit counts ac-  
 354 cumulated per grid cell. To mitigate sparsity, following Ouyang et al. (2018); Feng et al. (2020), the  
 355 top 25% frequently visited cells are retained for evaluation. For each of the four metrics, we form  
 356 a distribution from the generated trajectories and compare it against the ground truth distribution  
 357 using the Jensen-Shannon Divergence (JSD), following Zhu et al. (2023b); Wang et al. (2024).  
 358

359 **Implementation Details.** We primarily use GPT-4o-mini (2025-01-01-preview) (Achiam et al.,  
 360 2023) as the backbone for its capability–cost balance, with additional LLM evaluations reported in  
 361 Appendix H. Following Wang et al. (2024), we set the temperature to 0.1 to curb randomness, Top-p  
 362 to 1, and model trajectories at a 10-minute resolution. Grid size parameter  $S$  is set to 10.  $K$  is set to  
 363 3 to balance refinement quality and inference cost based on the parameter study in Appendix K. A  
 364 stability analysis verifying result consistency is provided in Appendix L.

## 365 6.2 QUANTITATIVE RESULTS

366 **Table 5** summarizes our main results, demonstrating ELLMob’s consistent superiority across all  
 367 event-driven settings. For instance, it improves the SI score by 32.3% for Typhoon Hagibis and the  
 368 SD score by 16.5% for the COVID-19 Pandemic compared to the strongest baselines. We observe  
 369 that LLM-based approaches generally outperform traditional deep learning models, particularly on  
 370 spatial coherence metrics (SD, SGD), benefiting from their ability to integrate event context. **Fur-  
 371 thermore, to verify spatial generalizability beyond the Tokyo area, we extended evaluations to Osaka**  
 372 **during the COVID-19 pandemic, with detailed results provided in Appendix I.**

373 The ablation study further dissects our ELLMob’s performance. Removing either the reflection mod-  
 374 ule (w/o I.A.&E.A.) or the event schema (w/o Eve. Ext.) consistently degrades performance. The  
 375 two components of the reflection module show distinct roles: Internal alignment (w/o E.A.) provides  
 376 foundational plausibility and external alignment (w/o I.A.) acts as a scenario-specific corrective. The  
 377 importance of external alignment is particularly evident during the COVID-19 Pandemic, where its  
 378 removal causes a catastrophic 132.4% performance degradation in the SI score. This highlights its  
 379 critical role in aligning with rational behaviors that substantially deviate from habitual patterns.

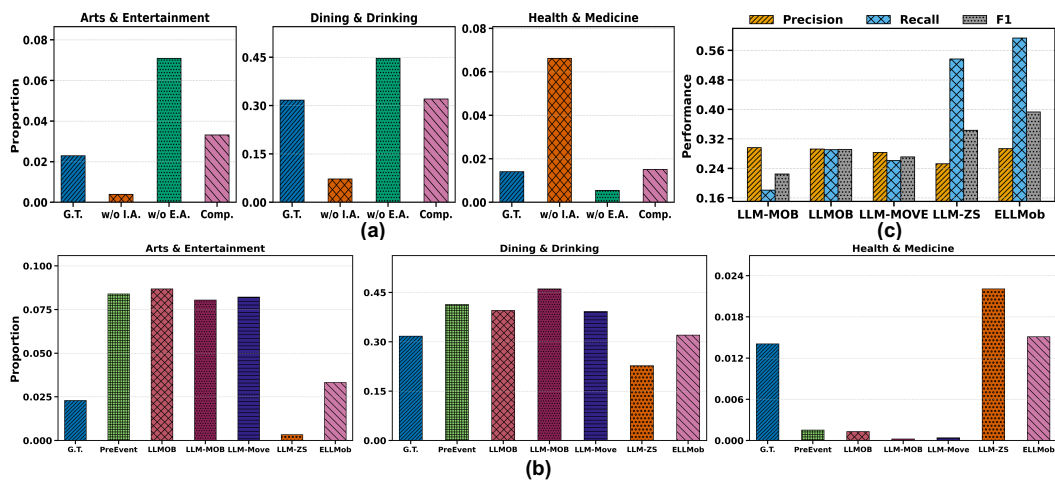


Figure 4: (a) Comparison of generated activity proportions (relative to the total number of activities) during the COVID-19 Pandemic. Each chart contrasts the ground truth (G.T.), distribution with: Without internal alignment (w/o I.A.), without external alignment (w/o E.A.), and the complete model (Comp.). (b) Comparison of three key activity categories distributions generated by ELLMob with various LLM-based baselines. (c) Performance comparison on the active user prediction task.

### 6.3 MODEL ANALYSIS

**Analysis of Self-alignment.** To dissect the distinct roles of internal and external alignment, we analyze the generated distributions of three sensitive top-categories (Arts & Entertainment, Dining & Drinking, and Health & Medicine) within the COVID-19 Pandemic. As shown in Figure 4 (a), removing either alignment leads to distinct failures. Lacking internal alignment, the model over-corrects for the event, generating an unrealistic surge in Health & Medicine while excessively suppressing Arts & Entertainment and Dining & Drinking activities. Conversely, without external alignment, the model rigidly adheres to habitual patterns, producing the opposite failure. Furthermore, Figure 4 (b) reveals that most LLM-based baselines default to habitual patterns (PreEvent) such as overestimating entertainment/dining while ignoring health-related travel, while LLM-ZS overcorrects by suppressing social activities entirely. Both extremes demonstrate that these baselines are unable to reconcile habitual patterns with event constraints in trajectory decision. The complete ELLMob successfully considers these two forces to produce a distribution that closely matches the ground truth, demonstrating the effectiveness of the self-alignment mechanism.

**Fundamental Decisions in Disasters.** Accurately identifying individuals who travel during extreme weather is critical for targeted early warnings and effective emergency response. We frame this as a binary classification task to identify a potentially high-risk cohort, which we define as the positive class of “active” users (at least one trip) during the typhoon. We evaluate LLM-based baselines for their strong ability to incorporate event context. As shown in Figure 4 (c), ELLMob achieves the highest F1-Score, driven by its superior recall of 59.3% in identifying this “active” high-risk population. This effectiveness is likely attributed to the iterative alignment process, which enhances LLM’s joint understanding of individual user mobility patterns and event constraints.

**Case Study.** To illustrate ELLMob’s reasoning process, Figure 5 presents a case study of a user with a strong culinary exploration pattern during the COVID-19 Pandemic. The initially planned trajectory (stay at home) over-aligns with the event’s public health constraints and is flagged by our reflection module for conflicting with the user’s habitual patterns. Guided by this internal feedback, the model iteratively refines the plan into a plausible trajectory that weighs both factors, ultimately limiting rather than eliminating dining outings. This case highlights the ELLMob’s ability to reconcile user patterns with event constraints to generate realistic behaviors that match the ground truth.

### 6.4 EVALUATION ON ROUTINE MOBILITY

To assess ELLMob’s generality, we evaluate its performance in routine scenarios. Since ELLMob is inherently event-driven, this evaluation requires defining a context for the normal period. We there-

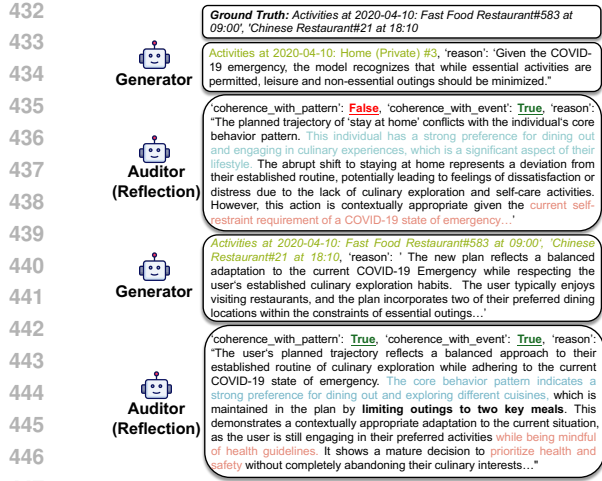


Figure 5: A case study of ELLMob’s workflow on the mobility of User No.003.

Table 6: Comparison of different methods under the Normal period with the best in **bold**.

Models	Normal period			
	SI↓	SD↓	CD↓	SGD↓
LSTM	0.1140	0.0696	0.0746	0.1499
DeepMove	0.1423	0.0428	0.0300	0.0742
GETNext	0.3071	0.1628	0.0126	0.0502
MHSA	0.1546	0.2346	0.0069	0.0269
TrajGAIL	0.0953	0.3432	0.0035	0.0104
DiffTraj	0.0748	0.1832	0.0361	0.0393
LLMOB	0.1460	0.1007	0.0051	0.0045
LLM-MOB	0.0654	0.0186	0.0059	0.0030
LLM-Move	0.1836	0.0261	0.0067	0.0036
LLM-ZS	0.0746	0.0311	0.0164	0.0027
ELLMob	<b>0.0496</b>	<b>0.0164</b>	<b>0.0025</b>	<b>0.0025</b>
w/o I.A.&E.A.	0.0639	0.0210	0.0041	0.0032
w/o I.A.	0.0545	0.0198	0.0026	0.0028
w/o E.A.	0.0556	0.0201	0.0037	0.0028

fore classify target days as either weekdays or weekends, defining their respective contexts by the typical societal operating status (e.g., differences in business hours, public transport schedules). As shown in Table 6, ELLMob outperforms all baselines. This confirms that the ELLMob’s alignment mechanisms are not narrowly tailored to disruptive events, but instead constitute a robust foundation that also excels in standard scenarios.

## 6.5 COMPARATIVE ABLATION ON ALIGNMENT STRATEGIES

Iterative-reflection methods such as Reflexion (Shinn et al., 2023), SELF-REFINE (Madaan et al., 2023), and Air (Liu et al., 2025) enhance LLM reasoning via self-correction, mainly targeting hallucinations or logical flaws in unstructured text. However, event-driven mobility requires resolving conflicts between habitual inertia and event-induced constraints. ELLMob introduces a methodological shift by grounding alignment in cognitive theory. At representation level, it replaces unstructured trajectories with structured decision variables to disentangle drivers. At decision level, rather than prompting the model to “improve” an answer, ELLMob employs dual-axis alignment to arbitrate competing objectives. This ensures trajectory adjustments are cognitively grounded rather than surface-level, locally reasonable fixes. To isolate the effectiveness of this design, we replaced ELLMob’s alignment module with each baseline strategy, while keeping all other settings identical. As the results shown in Table 7, ELLMob outperforms these variants in all metrics. This validates the necessity of the proposed alignment strategy for event-driven human mobility generation.

Table 7: Comparison with iterative-reflection baselines with the best performance in **bold**.

Models	Typhoon Hagibis				COVID-19 Pandemic				Tokyo 2021 Olympics			
	SI↓	SD↓	CD↓	SGD↓	SI↓	SD↓	CD↓	SGD↓	SI↓	SD↓	CD↓	SGD↓
Reflexion	0.1106	0.1282	0.0841	0.0855	0.1685	0.0588	0.0146	0.0269	0.1741	0.0308	0.0378	0.0704
SELF-REFINE	0.1979	0.0637	0.0135	0.0193	0.2122	0.1053	0.0344	0.0294	0.0826	0.0320	0.0073	0.0058
Air	0.0764	0.0710	0.0198	0.0204	0.1858	0.0454	0.0256	0.0291	0.0774	0.0441	0.0053	0.0035
ELLMob	<b>0.0642</b>	<b>0.0200</b>	<b>0.0041</b>	<b>0.0173</b>	<b>0.1003</b>	<b>0.0444</b>	<b>0.0080</b>	<b>0.0268</b>	<b>0.0617</b>	<b>0.0061</b>	<b>0.0022</b>	<b>0.0035</b>

## 6.6 COMPUTATIONAL EFFICIENCY

We evaluated computational overhead via token consumption and inference latency on a *per person per day* basis, with results in Table 8. Under GPT-4o-mini pricing, ELLMob uses 9,569 tokens and 18.68 seconds to generate one-day mobility for a single person, at \$0.00170. While this multi-stage architecture entails additional overhead compared to single-pass models, it demonstrates superior efficiency relative to generic reflection baselines like Reflexion (Shinn et al., 2023). This efficiency might stem from the integration of FTT, where structured alignment provides targeted guidance to

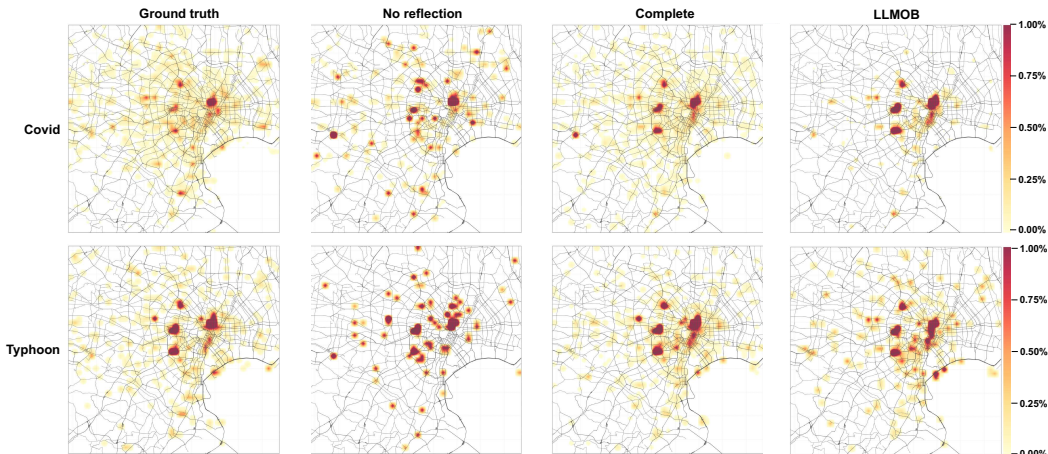
486  
487 Table 8: Computational Efficiency Analysis. The reported total token count includes both input and  
488 output tokens, and the overall cost is computed by accounting for their respective pricing rates.  
489

Model	Token Count	Inference Time (s)	Cost (USD)
LLMOB	1,271	10.12	0.00030
LLM-MOB	3,954	3.72	0.00064
LLM-MOVE	4,954	4.05	0.00078
LLM-ZS	5,184	3.34	0.00080
Reflexion	26,057	27.12	0.00417
SELF-REFINE	15,382	21.16	0.00258
Air	15,514	20.50	0.00260
ELLMob	9,569	18.68	0.00170

490  
491  
492  
493  
494  
495  
496  
497  
498  
499  
500 accelerate convergence and avoids the excessive resource cost of open-ended iterative refinement.  
501 Independent user-level generation allows parallelization, ensuring city-scale simulations feasible.  
502

## 503 6.7 VISUALIZATION OF SPATIAL MOBILITY PATTERNS

504  
505 Figure 6 presents heatmaps of the spatial mobility distribution during two high-impact events (Ty-  
506phoon Hagibis and the COVID-19 Pandemic), comparing ground truth against ELLMob, its ablated  
507version without the reflection module, and the strongest baseline LLMOB. Both our ablated model  
508and the strongest baseline LLMOB exhibit the core limitations of single-pass generation with im-  
509plicit trajectory decision, producing flawed spatial patterns: Excessive contraction during the ty-  
510phoon and incomplete decentralization during the COVID-19 Pandemic. In contrast, ELLMob’s  
511reflection module uses iterative alignment to achieve a fine-grained understanding of both user pat-  
512terns and event constraints, enabling it to reproduce realistic mobility patterns.  
513



520  
521  
522  
523  
524  
525  
526  
527  
528 Figure 6: Spatial mobility patterns. Darker red in the heatmaps indicates higher visit frequency.  
529  
530

## 531 7 CONCLUSION

532  
533 This work addresses the critical challenge of modeling human mobility during large-scale soci-  
534etal events. We contribute a comprehensive event-centric dataset covering three major events in  
535Tokyo and introduce ELLMob, a framework that explicitly reconciles competing mobility decisions  
536through gist-based alignment. Through extensive experiments, ELLMob demonstrates substantial  
537improvements over existing methods, enabling more reliable mobility generation for emergency  
538planning and urban management applications. However, we acknowledge that data from these plat-  
539forms may introduce demographic biases, such as skewing towards younger users, which is a com-  
mon limitation in LBSN research. Future work will aim to incorporate more diverse data sources.  
540

540 ETHICS STATEMENT  
541

542 All data used in our study is fully anonymized. The dataset was collected through Twitter Inc.’s Academic Research Product Track and Foursquare APIs in strict compliance with their privacy policies and terms of service. Our data collection and preprocessing methodology follows the established work (Yang et al., 2016). While the data sources are legitimate, we recognize that cross-referencing with original Twitter posts can potentially enable re-identification. To mitigate this risk, we implemented the following anonymization measures: (1) User IDs are replaced with random numbers; (2) Specific venue names are generalized to categories; (3) Exact timestamps are discretized into time intervals; and (4) User-generated comments are provided only in translated form to prevent linguistic fingerprinting. These comprehensive measures ensure that reverse identification is computationally infeasible even with access to the original platforms. Detailed descriptions of these privacy-preserving processes are included in the Appendix B.

553 REPRODUCIBILITY STATEMENT  
554

555 To ensure the reproducibility of our work, we have made our code and data publicly available in the supplementary materials. Our experimental setup, including evaluation metrics and parameter settings, are described in Section 6.1. Our data collection and filtering criteria are detailed in Appendix B.

560 REFERENCES  
561

562 Josh Achiam, Steven Adler, Sandhini Agarwal, Lama Ahmad, Ilge Akkaya, Florencia Leoni Ale-  
563 man, Diogo Almeida, Janko Altenschmidt, Sam Altman, Shyamal Anadkat, et al. Gpt-4 technical  
564 report. *arXiv preprint arXiv:2303.08774*, 2023.

565 Laura Alessandretti, Ulf Aslak, and Sune Lehmann. The scales of human mobility. *Nature*, 587  
566 (7834):402–407, 2020.

567 Shengnan An, Zexiong Ma, Zeqi Lin, Nanning Zheng, Jian-Guang Lou, and Weizhu  
568 Chen. Make your llm fully utilize the context. In A. Globerson, L. Mackey, D. Bel-  
569 grave, A. Fan, U. Paquet, J. Tomczak, and C. Zhang (eds.), *Advances in Neural In-  
570 formation Processing Systems*, volume 37, pp. 62160–62188. Curran Associates, Inc.,  
571 2024. URL [https://proceedings.neurips.cc/paper\\_files/paper/2024/file/71c3451f6cd6a4f82bb822db25cea4fd-Paper-Conference.pdf](https://proceedings.neurips.cc/paper_files/paper/2024/file/71c3451f6cd6a4f82bb822db25cea4fd-Paper-Conference.pdf).

572 Nabiha Asghar. Yelp dataset challenge: Review rating prediction. *arXiv preprint arXiv:1605.05362*,  
573 2016.

574 Ciro Beneduce, Bruno Lepri, and Massimiliano Luca. Large language models are zero-shot next  
575 location predictors. *IEEE Access*, 2025.

576 Enhui Chen, Yang Liu, and Min Yang. Revealing senior mobility patterns and activities in urban  
577 transit systems. *IEEE Transactions on Intelligent Transportation Systems*, 24(10):11424–11437,  
578 2023. doi: 10.1109/TITS.2023.3275389.

579 Eunjoon Cho, Seth A. Myers, and Jure Leskovec. Friendship and mobility: user movement in  
580 location-based social networks. In *Proceedings of the 17th ACM SIGKDD International Confer-  
581 ence on Knowledge Discovery and Data Mining*, KDD ’11, pp. 1082–1090, New York, NY, USA,  
582 2011. Association for Computing Machinery. ISBN 9781450308137. doi: 10.1145/2020408.  
583 2020579. URL <https://doi.org/10.1145/2020408.2020579>.

584 Seongjin Choi, Jiwon Kim, and Hwasoo Yeo. Trajgail: Generating urban vehicle trajectories using  
585 generative adversarial imitation learning. *Transportation Research Part C: Emerging Technolo-  
586 gies*, 2020. URL <https://api.semanticscholar.org/CorpusID:220936553>.

587 Chen Chu, Hengcai Zhang, Peixiao Wang, and Feng Lu. Simulating human mobility with a tra-  
588 jectory generation framework based on diffusion model. *International Journal of Geographical  
589 Information Science*, 38:847 – 878, 2024. URL <https://api.semanticscholar.org/CorpusID:267541591>.

594 DeepSeek-AI, Daya Guo, and et al. Deepseek-r1: Incentivizing reasoning capability in  
 595 llms via reinforcement learning. *ArXiv*, abs/2501.12948, 2025. URL <https://api.semanticscholar.org/CorpusID:275789950>.

597

598 Xiaoqi Duan, Tong Zhang, Zhibang Xu, Qiao Wan, Jinbiao Yan, Wangshu Wang, and You-  
 599 liang Tian. Discovering urban mobility structure: a spatio-temporal representational learning  
 600 approach. *International Journal of Digital Earth*, 16:4044 – 4072, 2023. URL <https://api.semanticscholar.org/CorpusID:263644586>.

601

602 Jie Feng, Yong Li, Chao Zhang, Funing Sun, Fanchao Meng, Ang Guo, and Depeng Jin. Deepmove:  
 603 Predicting human mobility with attentional recurrent networks. *WWW '18*, pp. 1459–1468, Re-  
 604 public and Canton of Geneva, CHE, 2018. International World Wide Web Conferences Steer-  
 605 ing Committee. ISBN 9781450356398. doi: 10.1145/3178876.3186058. URL <https://doi.org/10.1145/3178876.3186058>.

606

607 Jie Feng, Zeyu Yang, Fengli Xu, Haisu Yu, Mudan Wang, and Yong Li. Learning to simulate hu-  
 608 man mobility. In *Proceedings of the 26th ACM SIGKDD international conference on knowledge  
 609 discovery & data mining*, pp. 3426–3433, 2020.

610

611 Jie Feng, Yuwei Du, Jie Zhao, and Yong Li. Agentmove: A large language model based agentic  
 612 framework for zero-shot next location prediction. In *Proceedings of the 2025 Conference of  
 613 the Nations of the Americas Chapter of the Association for Computational Linguistics: Human  
 614 Language Technologies (Volume 1: Long Papers)*, pp. 1322–1338, 2025.

615

616 Shanshan Feng, Haoming Lyu, Fan Li, Zhu Sun, and Caishun Chen. Where to move next: Zero-  
 617 shot generalization of llms for next poi recommendation. In *2024 IEEE Conference on Artificial  
 618 Intelligence (CAI)*, pp. 1530–1535. IEEE, 2024.

619

620 Qiang Gao, Fan Zhou, Kunpeng Zhang, Goce Trajcevski, Xucheng Luo, and Fengli Zhang. Identify-  
 621 ing human mobility via trajectory embeddings. In *International Joint Conference on Artificial In-  
 622 telligence*, 2017. URL <https://api.semanticscholar.org/CorpusID:9552064>.

623

624 Qiang Gao, Goce Trajcevski, Fan Zhou, Kunpeng Zhang, Ting Zhong, and Fengli Zhang. Trajectory-based social circle inference. *Proceedings of the 26th ACM SIGSPATIAL Interna-  
 625 tional Conference on Advances in Geographic Information Systems*, 2018. URL <https://api.semanticscholar.org/CorpusID:53306139>.

626

627 Haofeng Gong, Xinning Zhu, Zheng Hu, and Jianzhou Diao. Two-stage trajectory generation model  
 628 for realistic human mobility simulation. *2023 IEEE International Conference on High Perfor-  
 629 mance Computing & Communications, Data Science & Systems, Smart City & Dependability in  
 630 Sensor, Cloud & Big Data Systems & Application (HPCC/DSS/SmartCity/DependSys)*, pp. 934–  
 631 941, 2023. URL <https://api.semanticscholar.org/CorpusID:268702859>.

632

633 Letian Gong, Yan Lin, Xinyue Zhang, Yiwen Lu, Xuedi Han, Yichen Liu, Shengnan Guo,  
 634 Youfang Lin, and Huaiyu Wan. Mobility-llm: Learning visiting intentions and travel prefer-  
 635 ence from human mobility data with large language models. In A. Globerson, L. Mackey,  
 636 D. Belgrave, A. Fan, U. Paquet, J. Tomczak, and C. Zhang (eds.), *Advances in Neu-  
 637 ral Information Processing Systems*, volume 37, pp. 36185–36217. Curran Associates, Inc.,  
 638 2024. URL [https://proceedings.neurips.cc/paper\\_files/paper/2024/file/3fb6c52aeb11e09053c16eabee74dd7b-Paper-Conference.pdf](https://proceedings.neurips.cc/paper_files/paper/2024/file/3fb6c52aeb11e09053c16eabee74dd7b-Paper-Conference.pdf).

639

640 Aaron Grattafiori, Abhimanyu Dubey, Abhinav Jauhri, Abhinav Pandey, Abhishek Kadian, Ahmad  
 641 Al-Dahle, Aiesha Letman, Akhil Mathur, Alan Schelten, Alex Vaughan, et al. The llama 3 herd  
 642 of models. *arXiv preprint arXiv:2407.21783*, 2024.

643

644 Sepp Hochreiter and Jürgen Schmidhuber. Long short-term memory. *Neural Comput.*, 9(8):  
 645 1735–1780, November 1997. ISSN 0899-7667. doi: 10.1162/neco.1997.9.8.1735. URL  
 646 <https://doi.org/10.1162/neco.1997.9.8.1735>.

647

648 Ye Hong, Yatao Zhang, Konrad Schindler, and Martin Raubal. Context-aware multi-head self-  
 649 attentional neural network model for next location prediction. *Transportation Research Part C:  
 650 Emerging Technologies*, 156:104315, 2023. ISSN 0968-090X. doi: <https://doi.org/10.1016/j.trc.2023.104315>. URL <https://www.sciencedirect.com/science/article/pii/S0968090X23003042>.

648 Jia Jia, Linghui Li, Pengfei Qiu, Binsi Cai, Xu Kang, Ximing Li, and Xiaoyong Li. Domain-  
 649 knowledge enhanced gans for high-quality trajectory generation. In *International Conference on*  
 650 *Intelligent Computing*, 2024. URL <https://api.semanticscholar.org/CorpusID:271770070>.

652 Chenlu Ju, Jiaxin Liu, Shobhit Sinha, Hao Xue, and Flora D. Salim. Trajilm: A modular llm-  
 653 enhanced agent-based framework for realistic human trajectory simulation. *Companion Proceed-  
 654 ings of the ACM on Web Conference 2025*, 2025. URL <https://api.semanticscholar.org/CorpusID:276617707>.

656 Joon-Seok Kim, Gautam Malviya Thakur, Licia Amichi, Annetta Burger, Chathika Gunaratne,  
 657 Joseph Tuccillo, Taylor Hauser, Joseph Bentley, Kevin Sparks, Debraj De, Chance Brown, Eliz-  
 658 abeth McBride, Jesse McGaha, James Gaboardi, Xiuling Nie, and Steven Carter Christopher.  
 659 Humonet: A framework for realistic modeling and simulation of human mobility network. In  
 660 *2024 25th IEEE International Conference on Mobile Data Management (MDM)*, pp. 185–194,  
 661 2024. doi: 10.1109/MDM1037.2024.00042.

663 Vaibhav Kulkarni and Benoît Garbinato. Generating synthetic mobility traffic using rnns. *Pro-  
 664 ceedings of the 1st Workshop on Artificial Intelligence and Deep Learning for Geographic  
 665 Knowledge Discovery*, 2017. URL <https://api.semanticscholar.org/CorpusID:28123397>.

667 Yang Li, Xudong Wang, Shuo Sun, Xiaolei Ma, and Guangquan Lu. Forecasting short-term subway  
 668 passenger flow under special events scenarios using multiscale radial basis function networks.  
 669 *Transportation Research Part C-emerging Technologies*, 77:306–328, 2017. URL <https://api.semanticscholar.org/CorpusID:114568637>.

671 Zhonghang Li, Lianghao Xia, Jiabin Tang, Yong Xu, Lei Shi, Long Xia, Dawei Yin, and Chao  
 672 Huang. Urbangpt: Spatio-temporal large language models. In *Proceedings of the 30th ACM  
 673 SIGKDD Conference on Knowledge Discovery and Data Mining*, KDD '24, pp. 5351–5362, New  
 674 York, NY, USA, 2024. Association for Computing Machinery. ISBN 9798400704901. doi: 10.  
 675 1145/3637528.3671578. URL <https://doi.org/10.1145/3637528.3671578>.

677 Yuebing Liang, Yichao Liu, Xiaohan Wang, and Zhan Zhao. Exploring large language mod-  
 678 els for human mobility prediction under public events. *Computers, Environment and Urban  
 679 Systems*, 112:102153, 2024. ISSN 0198-9715. doi: <https://doi.org/10.1016/j.compenvurbsys.2024.102153>. URL <https://www.sciencedirect.com/science/article/pii/S0198971524000826>.

682 Kai Liu, Zhihang Fu, Chao Chen, Wei Zhang, Rongxin Jiang, Fan Zhou, Yaowu Chen, Yue Wu,  
 683 and Jieping Ye. Enhancing llm's cognition via structurization. In A. Globerson, L. Mackey,  
 684 D. Belgrave, A. Fan, U. Paquet, J. Tomeczak, and C. Zhang (eds.), *Advances in Neural  
 685 Information Processing Systems*, volume 37, pp. 133710–133742. Curran Associates, Inc.,  
 686 2024. URL [https://proceedings.neurips.cc/paper\\_files/paper/2024/file/f169ec4d47933ea4896b994af8ff4f17-Paper-Conference.pdf](https://proceedings.neurips.cc/paper_files/paper/2024/file/f169ec4d47933ea4896b994af8ff4f17-Paper-Conference.pdf).

688 Wei Liu, Yancheng He, Yu Li, Hui Huang, Chengwei Hu, Jiaheng Liu, Shilong Li, Wenbo Su, and  
 689 Bo Zheng. AIR: Complex instruction generation via automatic iterative refinement. In Christos  
 690 Christodoulopoulos, Tanmoy Chakraborty, Carolyn Rose, and Violet Peng (eds.), *Proceedings of  
 691 the 2025 Conference on Empirical Methods in Natural Language Processing*, pp. 31952–31974,  
 692 Suzhou, China, November 2025. Association for Computational Linguistics. doi: 10.18653/  
 693 v1/2025.emnlp-main.1628. URL <https://aclanthology.org/2025.emnlp-main.1628/>.

695 Yingtao Luo, Q. Liu, and Zhaocheng Liu. Stan: Spatio-temporal attention network for next  
 696 location recommendation. *Proceedings of the Web Conference 2021*, 2021. URL <https://api.semanticscholar.org/CorpusID:231846408>.

698 Yuxiao Luo, Zhongcai Cao, Xin Jin, Kang Liu, and Ling Yin. Deciphering human mobil-  
 699 ity: Inferring semantics of trajectories with large language models. *2024 25th IEEE Interna-  
 700 tional Conference on Mobile Data Management (MDM)*, pp. 289–294, 2024. URL <https://api.semanticscholar.org/CorpusID:270123814>.

702 Aman Madaan, Niket Tandon, Prakhar Gupta, Skyler Hallinan, Luyu Gao, Sarah Wiegreffe, Uri  
 703 Alon, Nouha Dziri, Shrimai Prabhumoye, Yiming Yang, Sean Welleck, Bodhisattwa Prasad  
 704 Majumder, Shashank Gupta, Amir Yazdanbakhsh, and Peter Clark. Self-refine: Itera-  
 705 tive refinement with self-feedback. *ArXiv*, abs/2303.17651, 2023. URL <https://api.semanticscholar.org/CorpusID:257900871>.

706

707 Kun Ouyang, Reza Shokri, David S Rosenblum, and Wenzhuo Yang. A non-parametric generative  
 708 model for human trajectories. In *IJCAI*, volume 18, pp. 3812–3817, 2018.

709

710 Luca Pappalardo, Filippo Simini, Salvatore Rinzivillo, Dino Pedreschi, Fosca Giannotti, and Albert-  
 711 László Barabási. Returners and explorers dichotomy in human mobility. *Nature communications*,  
 712 6(1):8166, 2015.

713

714 V.F. Reyna and C.J. Brainerd. Fuzzy-trace theory: An interim synthesis. *Learning and Individual Differences*, 7(1):1–75, 1995. ISSN 1041-6080. doi: [https://doi.org/10.1016/1041-6080\(95\)90031-4](https://doi.org/10.1016/1041-6080(95)90031-4). URL <https://www.sciencedirect.com/science/article/pii/1041608095900314>. Special Issue: Fuzzy-Trace Theory.

715

716

717 Noah Shinn, Federico Cassano, Beck Labash, Ashwin Gopinath, Karthik Narasimhan, and Shunyu  
 718 Yao. Reflexion: language agents with verbal reinforcement learning. In *Neural Information  
 719 Processing Systems*, 2023. URL <https://api.semanticscholar.org/CorpusID:258833055>.

720

721

722 Xuan Song, Quanshi Zhang, Yoshihide Sekimoto, and Ryosuke Shibasaki. Prediction of human  
 723 emergency behavior and their mobility following large-scale disaster. In *Proceedings of the 20th  
 724 ACM SIGKDD international conference on Knowledge discovery and data mining*, pp. 5–14,  
 725 2014.

726

727 Xinyue Sun, Qingqing Ye, Haibo Hu, Yuandong Wang, Kai Huang, Tianyu Wo, and Jie Xu. Synthe-  
 728 sizing realistic trajectory data with differential privacy. *IEEE Transactions on Intelligent Trans-  
 729 portation Systems*, 24:5502–5515, 2023. URL <https://api.semanticscholar.org/CorpusID:256658156>.

730

731 Peizhi Tang, Chuang Yang, Tong Xing, Xiaohang Xu, Renhe Jiang, and Kaoru Sezaki. Instruction-  
 732 tuning llama-3-8b excels in city-scale mobility prediction. *Proceedings of the 2nd ACM SIGSPA-  
 733 TIAL International Workshop on Human Mobility Prediction Challenge*, 2024. URL <https://api.semanticscholar.org/CorpusID:273706998>.

734

735 Guowei Wang, Dongliang Liao, and Jing Li. Complete user mobility via user and trajectory em-  
 736 beddings. *IEEE Access*, 6:72125–72136, 2018. URL <https://api.semanticscholar.org/CorpusID:56170111>.

737

738 Jiawei Wang, Renhe Jiang, Chuang Yang, Zengqing Wu, Makoto Onizuka, Ryosuke Shibasaki,  
 739 Noboru Koshizuka, and Chuan Xiao. Large language models as urban residents: An LLM agent  
 740 framework for personal mobility generation. In *The Thirty-eighth Annual Conference on Neu-  
 741 ral Information Processing Systems*, 2024. URL <https://openreview.net/forum?id=1iHmhMHNyA>.

742

743 Xinglei Wang, Meng Fang, Zichao Zeng, and Tao Cheng. Where would i go next? large language  
 744 models as human mobility predictors. *arXiv preprint arXiv:2308.15197*, 2023.

745

746 Xingrui Wang, Xinyu Liu, Ziteng Lu, and Hanfang Yang. Large scale gps trajectory generation  
 747 using map based on two stage gan. *Journal of Data Science*, 2021. URL <https://api.semanticscholar.org/CorpusID:234169684>.

748

749 Hao Xue, Bhanu Prakash Voutharoja, and Flora D. Salim. Leveraging language foundation models  
 750 for human mobility forecasting. *Proceedings of the 30th International Conference on Advances  
 751 in Geographic Information Systems*, 2022. URL <https://api.semanticscholar.org/CorpusID:252212309>.

752

753 Dingqi Yang, Daqing Zhang, Vincent W. Zheng, and Zhiyong Yu. Modeling user activity preference  
 754 by leveraging user spatial temporal characteristics in lbsns. *IEEE Transactions on Systems, Man,  
 755 and Cybernetics: Systems*, 45(1):129–142, 2015. doi: 10.1109/TSMC.2014.2327053.

756 Dingqi Yang, Daqing Zhang, and Bingqing Qu. Participatory cultural mapping based on collective  
 757 behavior data in location-based social networks. *ACM Trans. Intell. Syst. Technol.*, 7(3), January  
 758 2016. ISSN 2157-6904. doi: 10.1145/2814575. URL <https://doi.org/10.1145/2814575>.  
 759

760 Dingqi Yang, Bingqing Qu, Jie Yang, and Philippe Cudre-Mauroux. Revisiting user mobility  
 761 and social relationships in lbsns: A hypergraph embedding approach. In *The World Wide Web  
 762 Conference, WWW '19*, pp. 2147–2157, New York, NY, USA, 2019. Association for Com-  
 763 puting Machinery. ISBN 9781450366748. doi: 10.1145/3308558.3313635. URL <https://doi.org/10.1145/3308558.3313635>.  
 764

765 Qwen An Yang, Baosong Yang, Beichen Zhang, Binyuan Hui, Bo Zheng, Bowen Yu, Chengyuan  
 766 Li, Dayiheng Liu, Fei Huang, Guanting Dong, Haoran Wei, Huan Lin, Jian Yang, Jianhong Tu,  
 767 Jianwei Zhang, Jianxin Yang, Jiaxin Yang, Jingren Zhou, Junyang Lin, Kai Dang, Keming Lu,  
 768 Keqin Bao, Kexin Yang, Le Yu, Mei Li, Mingfeng Xue, Pei Zhang, Qin Zhu, Rui Men, Runji  
 769 Lin, Tianhao Li, Tingyu Xia, Xingzhang Ren, Xuancheng Ren, Yang Fan, Yang Su, Yi-Chao  
 770 Zhang, Yunyang Wan, Yuqi Liu, Zeyu Cui, Zhenru Zhang, Zihan Qiu, Shanghaoran Quan, and  
 771 Zekun Wang. Qwen2.5 technical report. *ArXiv*, abs/2412.15115, 2024. URL <https://api.semanticscholar.org/CorpusID:274859421>.  
 772

773 Song Yang, Jiamou Liu, and Kaiqi Zhao. Getnext: Trajectory flow map enhanced transformer  
 774 for next poi recommendation. In *Proceedings of the 45th International ACM SIGIR Conference  
 775 on Research and Development in Information Retrieval, SIGIR '22*, pp. 1144–1153, New York,  
 776 NY, USA, 2022. Association for Computing Machinery. ISBN 9781450387323. doi: 10.1145/  
 777 3477495.3531983. URL <https://doi.org/10.1145/3477495.3531983>.  
 778

779 Kunyi Zhang, Yanbo Pang, Yurong Zhang, and Yoshihide Sekimoto. Mobglm: A large lan-  
 780 guage model for synthetic human mobility generation. *Proceedings of the 32nd ACM Inter-  
 781 national Conference on Advances in Geographic Information Systems*, 2024. URL <https://api.semanticscholar.org/CorpusID:274187355>.  
 782

783 Kefan Zhao and Nana Wang. Generating spatiotemporal trajectories with gans and conditional gans.  
 784 In *International Conference on Neural Information Processing*, 2023. URL <https://api.semanticscholar.org/CorpusID:265455724>.  
 785

786 Yu Zheng, Lizhu Zhang, Xing Xie, and Wei-Ying Ma. Mining interesting locations and travel  
 787 sequences from gps trajectories. In *Proceedings of the 18th International Conference on World  
 788 Wide Web, WWW '09*, pp. 791–800, New York, NY, USA, 2009. Association for Computing  
 789 Machinery. ISBN 9781605584874. doi: 10.1145/1526709.1526816. URL <https://doi.org/10.1145/1526709.1526816>.  
 790

791 Xiaofeng Zhong, Yinfeng Xiang, Fang Yi, Chao Li, and Qinmin Yang. Hmp-llm: Human  
 792 mobility prediction based on pre-trained large language models. In *2024 IEEE 4th Interna-  
 793 tional Conference on Digital Twins and Parallel Intelligence (DTPI)*, pp. 687–692, 2024. doi:  
 794 10.1109/DTPI61353.2024.10778764.  
 795

796 Yuanshao Zhu, Yongchao Ye, Ying Wu, Xiangyu Zhao, and James Yu. Synmob: Creating  
 797 high-fidelity synthetic gps trajectory dataset for urban mobility analysis. In A. Oh, T. Naumann,  
 798 A. Globerson, K. Saenko, M. Hardt, and S. Levine (eds.), *Advances in Neural Infor-  
 799 mation Processing Systems*, volume 36, pp. 22961–22977. Curran Associates, Inc., 2023a.  
 800 URL [https://proceedings.neurips.cc/paper\\_files/paper/2023/file/4786c0d1b9687a841bc579b0b8b01b8e-Paper-Datasets\\_and\\_Benchmarks.pdf](https://proceedings.neurips.cc/paper_files/paper/2023/file/4786c0d1b9687a841bc579b0b8b01b8e-Paper-Datasets_and_Benchmarks.pdf).  
 801

802 Yuanshao Zhu, Yongchao Ye, Shiya Zhang, Xiangyu Zhao, and James Yu. Difftraj: Gener-  
 803 ating GPS trajectory with diffusion probabilistic model. In *Thirty-seventh Conference on Neural  
 804 Information Processing Systems*, 2023b. URL <https://openreview.net/forum?id=ykMdzevPkJ>.  
 805

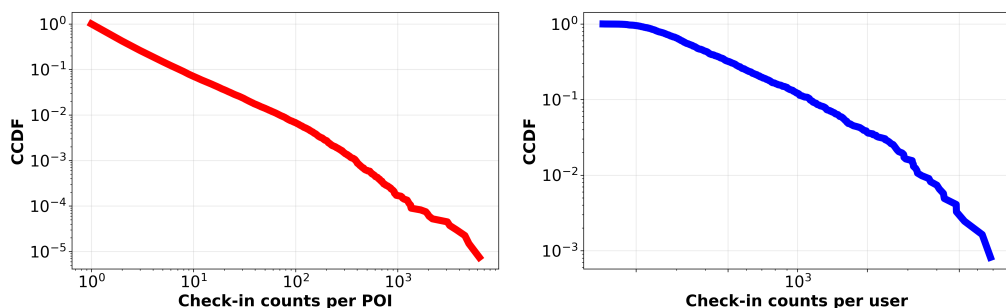
810 A USE OF LARGE LANGUAGE MODELS  
811

812 We employed LLMs for grammar checking and polishing the English expression throughout this  
813 manuscript. It is important to note that while our research focuses on leveraging LLMs for human  
814 mobility modeling, the LLMs studied in this work are the subject of our research rather than tools for  
815 research ideation or scientific writing. All experimental design, analysis, and scientific conclusions  
816 were developed independently by the authors.

817  
818 B DATA COLLECTION, CLEANING AND ANONYMIZATION  
819

820 **Data Collection.** The raw data used in this study are derived from Foursquare check-in records  
821 that users publicly synced to Twitter, which are accessible through the Twitter API. We first used  
822 the Twitter API to identify users who were active within a 100 km radius of Tokyo Station during  
823 April 2021, and then retrieved all of their tweets from 2019 to 2021. We subsequently identified  
824 Foursquare check-in tweets (auto-posted via the Foursquare→Twitter integration) and extracted the  
825 associated metadata, including the Point-of-Interest (POI) name, category, and subcategory<sup>1</sup>, geo-  
826 graphic coordinates (latitude & longitude), timestamp, and user-provided comment text. The ex-  
827 tracted check-ins served as the raw dataset for this study. Importantly, these user-level records span  
828 2019 to 2021, providing a longitudinal dataset that captures diverse social and environmental con-  
829 texts, including but not limited to the Typhoon Hagibis, COVID-19 pandemic, and the Tokyo 2021  
830 Olympics, which collectively form the foundation of this study.

831 **Data Cleaning.** After obtaining the raw dataset, we performed several cleaning steps to improve  
832 data quality. First, we discarded users with missing check-ins for an entire year. Next, we parsed  
833 geographic coordinates to obtain prefecture information and assigned each user to their most fre-  
834 quently visited one. For example, users whose check-ins were primarily in Tokyo were labeled as  
835 “Tokyo users”. We filtered the dataset to include only Tokyo users for two primary reasons: To  
836 ensure a homogeneous dataset by mitigating confounding variables from adjacent prefectures and to  
837 leverage the wide spectrum of mobility behaviors characteristic of a global mega city. Furthermore,  
838 check-ins showing abrupt, unrealistic location changes (e.g., from Tokyo to Okinawa within a short  
839 time frame) were removed to mitigate data drift, following the criteria adopted by Yang et al. (2016).  
840 Finally, we retained only users with consistently dense check-in activity throughout the study pe-  
841 riod, yielding a final dataset of 1,100 users and 567,080 check-ins. As illustrated in Figure A2, the  
842 check-in distribution of these sampled users follows a power-law characteristic, which is consistent  
843 with real-world human activity patterns (Yang et al., 2019).



844  
845  
846  
847  
848  
849  
850  
851  
852  
853  
854  
855 Figure A2: Log-log plots of the Complementary Cumulative Distribution Function (CCDF) of  
856 check-in counts. Left part of the figure shows the distribution of check-ins per POI. Left part of  
857 the figure shows the distribution of check-ins per user. Both distributions exhibit a linear trend,  
858 characteristic of a power-law.  
859

860 **Data Anonymization.** To protect privacy, we applied deterministic, one-way pseudonymization to  
861 all identifiers. Twitter user IDs were irreversibly mapped to integer surrogates, and POI identifiers  
862 were processed in the same manner. POI names (e.g., “Yoshinoya Shinjuku”) were removed while  
863

<sup>1</sup><https://docs.foursquare.com/data-products/docs/categories>

864 retaining only category information (e.g., major category “Dining and Drinking” and subcategory  
 865 “Donburi Restaurant”).

866 Further details are available in the supplementary materials, which include a portion of the raw data  
 867 and the source code.

## 870 C MOBILITY DATA SAMPLE

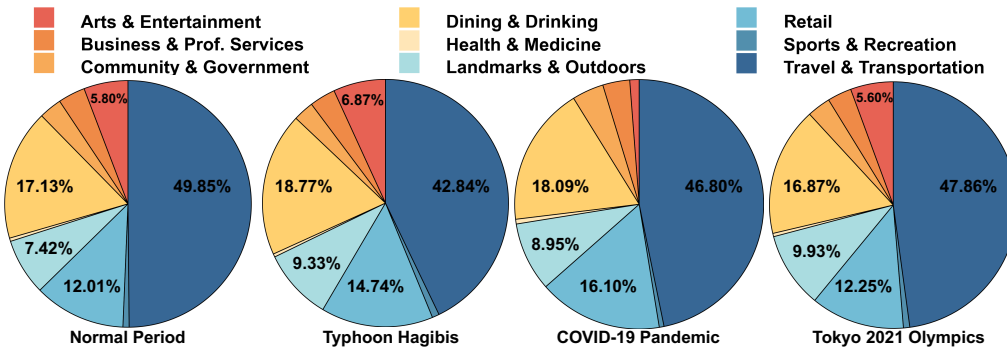
872 To provide a concrete illustration of the processed user activity trajectories used in our analysis,  
 873 [Table A2](#) presents an exemplary sequence from a single user. This sample highlights the data struc-  
 874 ture, integrating precise spatio-temporal features (latitude, longitude, time) with functional seman-  
 875 tics (Location Name, Category), which forms the foundation for our mobility analysis.

877 Table A2: A user’s mobility sample, showcasing activity trajectories with spatio-temporal features  
 878 and comments.

User	Lat.	Long.	Subcategory	Sub. ID	Category	Timestamp	Comments (Translated)
0022	35.652	139.543	Home Appliance Store	65	Retail	2020-04-07 18:40	Done with work! Chofu tan says a state of emergency has been declared.
0022	35.633	139.578	Clothing Store	542	Retail	2020-04-10 19:20	For coronavirus prevention, credit cards are now self-scan (this is ideal).
0022	35.632	139.578	Rail Station	2422	Travel & Transport	2020-04-10 19:30	But wait, isn’t this still considered close contact?

## 888 D BEHAVIOR DISTRIBUTION

891 [Figure A3](#) shows that different events impose distinct mobility behavior. For instance, Typhoon  
 892 Hagibis disrupts transportation, leading to widespread cancellations. Similarly, the declaration of  
 893 COVID-19 Pandemic canceled nearly all entertainment activities due to self-quarantine require-  
 894 ments.



907 Figure A3: A visualization of category distributions across four event scenarios. Each data point  
 908 represents the percentage share of the category out of the total activities in that scenario.

## 911 E EVENT SCHEMA

914 This section provides three complete instances of the event schema introduced in the main paper  
 915 (Typhoon Hagibis, Tokyo 2021 Olympics, and COVID-19 Pandemic). Each instance follows the  
 916 same four aspect structure used to derive the event context  $E_{ctx}$  from raw text  $E_c$ . The content is  
 917 shown in [Figure A4](#). Furthermore, this structured approach is highly extensible, allowing for the  
 integration of custom information to generate tailored outputs for any given event.

918

**Event Schema of Typhoon Hagibis:**

919

**Event Profile:** Typhoon Hagibis struck the Tokyo metropolitan area on October 12, 2019.

920

**Intensity & Scale:** The typhoon reached Category 5 strength, bringing violent winds and heavy rainfall, with Tokyo recording over 240 mm of rain in 24 hours.

921

**Infrastructure & Service Impact:** More than 370,000 homes experienced power outages, leading to the suspension of all major transportation services and closure of popular attractions.

922

**Official Directives:** Authorities issued evacuation orders to over 800,000 households and urged approximately six million residents to stay indoors and monitor official advisories.

923

924

925

**Event Schema of COVID-19 Pandemic:**

926

**Event Profile:** The COVID-19 state of emergency declared by Prime Minister Shinzo Abe under Article 32 of the Act on Special Measures for Pandemic Influenza and New Infectious Diseases. The state of emergency covered Tokyo, Saitama, Chiba, Kanagawa, Osaka, Hyogo, and Fukuoka.

927

**Intensity & Scale:** It did not entail a full lockdown but allowed prefectural governors to request residents to stay home for essential activities.

928

**Infrastructure & Service Impact:** Essential services like grocery stores, pharmacies, banks, public transport, and utilities were asked to continue operating with infection-control measures. Large commercial and entertainment facilities were requested to suspend or restrict operations.

929

**Official Directives:** Prefectural governors were authorized to request residents to stay home except for essentials like medical visits, shopping, or commuting. Non-compliant businesses could have their names disclosed.

930

931

932

933

934

**Event Schema of Tokyo 2021 Olympics:**

935

**Event Profile:** The 'Tokyo 2021 Olympics', starting from July 23, in Tokyo, Japan.

936

**Intensity & Scale:** Significant traffic jams occurred in and around central Tokyo and Olympic venues due to with separate area lockdowns imposed by organizers and construction restricted access near venues. A notable but limited increase in travel to regional tourist destinations during the holiday period.

937

**Infrastructure & Service Impact:** Public transportation saw reduced usage, while regional tourist infrastructure experienced a temporary uptick in visitors. However, overall tourism sector recovery remained incomplete compared to pre-pandemic levels.

938

**Official Directives:** Government advisories 'stay at home' measures during the COVID-19 state of emergency, targeting the population of Tokyo and surrounding areas.

939

940

941

942

943

Figure A4: This figure shows three event schema instances (Typhoon Hagibis, COVID-19 pandemic, and Tokyo 2021 Olympics), serving as structured contexts for event-driven mobility generation.

944

**Algorithm 1 ELLMob: trajectory generation under event**

945

**Require:** long-term data  $D_{\text{hist}}$ , short-term data  $D_{\text{short-term}}$ , event context  $E_c$ , max iters  $N_{\text{max}}$ 

946

**Ensure:** Event-aware trajectory  $\tau_{\text{final}}$ 

947

1:  $E_{\text{ctx}} \leftarrow \text{EVENTSCHEMACONSTRUCTION}(E_c)$ 

948

2:  $G_{\text{pat}} \leftarrow \text{EXTRACTPATTERNGIST}(D_{\text{hist}}, D_{\text{short-term}})$ 

949

3:  $G_{\text{evt}} \leftarrow \text{EXTRACTEVENTGIST}(E)_{\text{ctx}}$ 

950

4:  $\text{Feedback} \leftarrow \text{NONE}$ ,  $\tau_{\text{prev}} \leftarrow \text{NONE}$ 

951

5: **for**  $i = 1$  to  $N_{\text{max}}$  **do**

952

6:     **if**  $\text{Feedback} = \text{NONE}$  **then**

953

7:          $(\tau, \text{Justification}) \leftarrow \text{GENERATEINITIALTRAJECTORY}(D_{\text{hist}}, D_{\text{short-term}}, E_{\text{ctx}})$ 

954

8:     **else**

955

9:          $(\tau, \text{Justification}) \leftarrow$ 

956

10:          $\text{REGENERATETRAJECTORY}(D_{\text{hist}}, D_{\text{short-term}}, E_{\text{ctx}}, \tau_{\text{prev}}, \text{Feedback})$ 

957

11:     **end if**

958

12:      $G_{\text{act}} \leftarrow \text{EXTRACTACTIONGIST}(\tau, \text{Justification})$ 

959

13:      $(\text{Alignment}, \text{Feedback}) \leftarrow \text{AUDITALIGNMENT}(G_{\text{act}}, G_{\text{pat}}, G_{\text{evt}})$ 

960

14:     **if**  $\text{Alignment}$  **then**

961

15:          $\tau_{\text{final}} \leftarrow \tau$ 

▷ Accept

962

16:         **return**  $\tau_{\text{final}}$ 

963

17:     **end if**

964

18:      $\tau_{\text{prev}} \leftarrow \tau$ 

▷ Last candidate

965

19:      $\tau_{\text{final}} \leftarrow \tau$ 

966

20:     **return**  $\tau_{\text{final}}$ 

967

968

969

970

971

## 972 F COMPONENT ANALYSIS OF FTT

974 To verify the concrete impact of FTT-guided design choices, we conducted additional ablation studies:  
 975 A variant that relies mainly on raw features (verbatim) without gist abstraction (w/ verbatim),  
 976 and a variant that removes the bottom-line gist component, using generic summaries instead (w/o  
 977 bottom-line). As shown in Table A3, ELLMob consistently outperforms these variants across all  
 978 event scenarios. These results confirm that the FTT-guided framework concretely improves genera-  
 979 tion quality under event-driven mobility.

980  
 981 Table A3: Ablation study on the effectiveness of different FTT components with the best perfor-  
 982 mance highlighted in **bold**.

984 <b>Models</b>	985 <b>Typhoon Hagibis</b>				986 <b>COVID-19 Pandemic</b>				987 <b>Tokyo 2021 Olympics</b>			
	988 SI↓	SD↓	CD↓	SGD↓	SI↓	SD↓	CD↓	SGD↓	SI↓	SD↓	CD↓	SGD↓
w/ verbatim	0.1511	0.0724	0.0230	0.0595	0.2071	0.0713	0.0324	0.0422	0.1030	0.0452	0.0054	0.0189
w/o bottom	0.0978	0.0443	0.0101	0.0327	0.1687	0.0690	0.0305	0.0333	0.0892	0.0364	0.0036	0.0082
ELLMob	<b>0.0642</b>	<b>0.0200</b>	<b>0.0041</b>	<b>0.0173</b>	<b>0.1003</b>	<b>0.0444</b>	<b>0.0080</b>	<b>0.0268</b>	<b>0.0617</b>	<b>0.0061</b>	<b>0.0022</b>	<b>0.0035</b>

## 990 G ALGORITHM PSEUDO-CODES

991 To clearly present the proposed framework, we outline the event-driven trajectory generation process  
 992 of ELLMob. This procedure integrates long-term and short-term mobility records with structured  
 993 event contexts, iteratively generating and auditing candidate trajectories until a satisfactory align-  
 994 ment with mobility patterns and event-specific constraints is achieved. Algorithm 1 summarizes  
 995 the key steps, from constructing the event schema and extracting representative gists to producing,  
 996 evaluating, and refining trajectories under feedback-guided auditing.

## 1000 H ROBUSTNESS ACROSS ARCHITECTURES

1001 To verify that the superior performance of ELLMob is intrinsic to our cognitive framework rather  
 1002 than dependent on the specific LLM, we conducted a comparative evaluation using Gemini Flash 2.0  
 1003 as the uniform backbone for all methods. As detailed in Table A4, ELLMob maintains the lowest  
 1004 JSD scores across all event scenarios, mirroring its superior performance on previous benchmarks.  
 1005 In contrast, baseline methods exhibit volatility when subjected to this backbone shift. For instance,  
 1006 the SI of LLM-MOB deteriorates markedly from 0.1214 to 0.3180 in the Typhoon Hagibis, indi-  
 1007 cating a strong dependency of the specific backbone. This divergence highlights that while baseline  
 1008 performance is often contingent on model-specific characteristics, ELLMob effectively captures mo-  
 1009 bility patterns through explicit cognitive alignment, ensuring consistent superiority independent of  
 1010 the proprietary backbone.

1011 To further substantiate the robustness and reproducibility of our framework, we extended the exper-  
 1012 imental evaluation to include three representative open-source large language models: LLaMA3-8B  
 1013 (Grattafiori et al., 2024), Qwen-2.5-14B (Yang et al., 2024), and DeepSeek-R1-Distill-Qwen-7B  
 1014 (R1-Q7B) (DeepSeek-AI et al., 2025). This expansion mitigates concerns regarding the reliance on  
 1015 proprietary APIs and confirms the adaptability of the method to local computing environments. As  
 1016 presented in Table A5, ELLMob achieves consistent alignment performance across these diverse  
 1017 backbones. The effectiveness on open-source LLMs confirms that the capability of ELLMob stems  
 1018 from the cognitive alignment strategy rather than the inherent capacity of the underlying model.

## 1019 I REGIONAL GENERALIZABILITY EVALUATION

1020 The primary experiments in the main text focus on the Tokyo metropolitan area. To verify that  
 1021 ELLMob generalizes to other geographical contexts and is not overfitted to a specific urban layout,  
 1022 we extended our evaluation to Osaka. We constructed a new dataset comprising 1,100 users during  
 1023 the COVID-19 pandemic, maintaining a scale consistent with the Tokyo dataset. Table A6 presents

1026  
1027 Table A4: Performance comparison of different methods using Gemini Flash 2.0. Performance is  
1028 evaluated by JSD across four dimensions with the best performance highlighted in **bold**.  
1029

1030 <b>Models</b>	1031 <b>Typhoon Hagibis</b>				1032 <b>COVID-19 Pandemic</b>				1033 <b>Tokyo 2021 Olympics</b>			
	1034 SI↓	1035 SD↓	1036 CD↓	1037 SGD↓	1038 SI↓	1039 SD↓	1040 CD↓	1041 SGD↓	1042 SI↓	1043 SD↓	1044 CD↓	1045 SGD↓
LLMOB	0.1069	0.0743	0.0126	0.0196	0.0846	0.0693	0.0105	0.0292	0.0572	0.0281	0.0031	0.0087
LLM-MOB	0.3180	0.1726	0.2004	0.0968	0.1428	0.0660	0.0280	0.0459	0.0379	0.0154	0.0053	0.0065
LLM-Move	0.2383	0.0721	0.0887	0.0465	0.3683	0.0644	0.0378	0.0353	0.1979	0.0287	0.0097	0.0063
LLM-ZS	0.3466	0.1537	0.2556	0.1084	0.2788	0.1344	0.2489	0.1479	0.0967	0.0313	0.0137	0.0057
ELLMob	<b>0.0850</b>	<b>0.0267</b>	<b>0.0087</b>	<b>0.0160</b>	<b>0.0546</b>	<b>0.0586</b>	<b>0.0069</b>	<b>0.0210</b>	<b>0.0113</b>	<b>0.0074</b>	<b>0.0016</b>	<b>0.0048</b>

1036  
1037 Table A5: Performance comparison of ELLMob across different open-source LLM backbones. Per-  
1038 formance is evaluated by JSD across four dimensions  
1039

1040 <b>Models</b>	1041 <b>Typhoon Hagibis</b>				1042 <b>COVID-19 Pandemic</b>				1043 <b>Tokyo 2021 Olympics</b>			
	1044 SI↓	1045 SD↓	1046 CD↓	1047 SGD↓	1048 SI↓	1049 SD↓	1050 CD↓	1051 SGD↓	1052 SI↓	1053 SD↓	1054 CD↓	1055 SGD↓
LLaMA3-8B	0.0663	0.0512	0.0004	0.0132	0.0669	0.0624	0.0087	0.0263	0.0407	0.0322	0.0023	0.0030
Qwen-2.5-14B	0.1594	0.0607	0.0091	0.0115	0.0836	0.0646	0.0016	0.0225	0.0530	0.0238	0.0035	0.0021
R1-Q7B	0.0881	0.0516	0.0033	0.0203	0.1104	0.0993	0.0163	0.0392	0.0570	0.0251	0.0015	0.0071

1045  
1046 the performance comparison against baseline methods, where ELLMob consistently outperforms all  
1047 competitors. This result demonstrates its adaptability to diverse urban layouts beyond Tokyo.  
1048

## 1049 J EVENT GENERALIZABILITY EVALUATION

1050 The primary experiments in the main text focus on events characterized by external restrictions or  
1051 exogenous shocks. To verify that ELLMob generalizes to traditional cultural festivities that induce  
1052 distinct, voluntarily driven deviation patterns, we extended our evaluation to the New Year scenario.  
1053 Table A7 presents the performance comparison against baseline methods. ELLMob consistently  
1054 outperforms baselines across all metrics, demonstrating its capability to model diverse event types.  
1055

1056 **Discussion of Event Scalability.** The scalability of ELLMob stems from its ability to generalize  
1057 across distinct event semantics rather than overfitting to specific scenarios. The Event Schema  
1058 module converts diverse narratives into standardized semantic descriptors (e.g., traffic impact), creating a  
1059 universal conflict-resolution logic via the FTT-based alignment. To rigorously verify this generaliza-  
1060 tion, selected four events represent diverse and contrasting typologies along three key dimensions:  
1061

- 1062 • Restrictive vs. Promotive: COVID-19 Pandemic and Typhoon Hagibis restrict movement, whereas  
1063 the New Year scenario promotes social gatherings.
- 1064 • Stochastic vs. Periodic: Typhoon Hagibis is unpredictable and sudden, while New Year's is peri-  
1065 odic and cyclic.
- 1066 • Global vs. Local (Hybrid): The COVID-19 Pandemic affects the entire city globally, whereas the  
1067 Tokyo 2021 Olympics imposes hybrid constraints concentrated in specific zones.

1068 Notably, we applied the identical framework and parameter settings across all scenarios. The consis-  
1069 tent performance across these contrasting types confirms that ELLMob can capture the underlying  
1070 logic of event-driven mobility. While extensive empirical validation is currently constrained by the  
1071 scarcity of high-quality event-mobility data in the community, this work, to the best of our knowl-  
1072 edge, is the first attempt to validate scalability across a wide spectrum of distinct event types.  
1073

## 1074 K PARAMETER SENSITIVE STUDY OF ITERATION

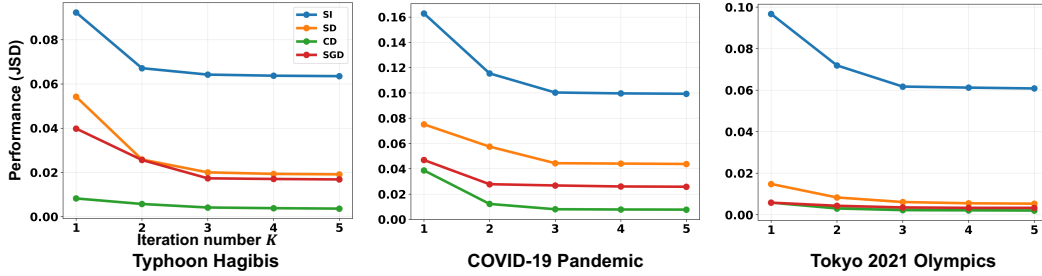
1075 As shown in Figure A5, performance improves substantially in the first three iterations with only  
1076 marginal gains thereafter, justifying our choice of K=3 as an effective trade-off between refinement  
1077 quality and computational cost.

1080 Table A6: Regional generalizability analysis on the Osaka data during the COVID-19 Pandemic.  
 1081 Performance is evaluated by JSD across four dimensions with the best performance in **bold**.  
 1082

Model	SI	SD	CD	SGD
LLMOB	0.1934	0.1589	0.0344	0.1201
LLM-MOB	0.1732	0.1617	0.0304	0.0988
LLM-MOVE	0.2134	0.1555	0.0698	0.1227
LLM-ZS	0.1531	0.1788	0.0299	0.1161
<b>ELLMob</b>	<b>0.1131</b>	<b>0.1001</b>	<b>0.0120</b>	<b>0.0556</b>

1090 Table A7: Event generalizability analysis on the New Year scenario in Tokyo. Performance is  
 1091 evaluated by JSD across four dimensions with the best performance in **bold**.  
 1092

Model	SI	SD	CD	SGD
LLMOB	0.0776	0.0391	0.0230	0.0422
LLM-MOB	0.1061	0.0413	0.0318	0.0379
LLM-MOVE	0.2248	0.0493	0.0272	0.0550
LLM-ZS	0.0996	0.0497	0.0230	0.0481
<b>ELLMob</b>	<b>0.0598</b>	<b>0.0250</b>	<b>0.0200</b>	<b>0.0317</b>



1101 Figure A5: Performance comparison across iteration numbers  $K = 1$  to 5 for three major events:  
 1102 Typhoon Hagibis, COVID-19 Pandemic, and Tokyo 2021 Olympics. Performance is measured using  
 1103 Jensen-Shannon Divergence (JSD), where lower values indicate better performance.  
 1104  
 1105  
 1106  
 1107  
 1108  
 1109  
 1110  
 1111

## L STABILITY ANALYSIS

1112 Given the inherent stochastic nature of LLMs, generated outputs may vary across different runs with  
 1113 the same input. To verify the robustness of our approach, we conducted repeated experiments across  
 1114 5 distinct random seeds with the results shown in Table A8, Table A9, Table A10. As indicated by the  
 1115 standard deviations, ELLMob consistently maintains high stability across different initializations.  
 1116 These results demonstrate that while absolute performance may vary, ELLMob provides statistically  
 1117 consistent predictions and is less sensitive to random seed variations.

## M PROMPT

1118 This appendix details the sequence of prompts utilized within the ELLMob framework. These  
 1119 prompts work in concert to guide the LLM through the entire process, from initial data process-  
 1120 ing to the final reflective generation of mobility trajectories.

1121 **Event context generation.** To enable the LLM to interpret unstructured event descriptions, the  
 1122 following prompt is used to transform raw text into a structured intelligence brief. It instructs the  
 1123 model to act as an analyst, extracting key details and their implications for public behavior.

1134 Table A8: Stability analysis on the Typhoon Hagibis dataset. Results are reported as Mean  $\pm$   
1135 Standard Deviation across 5 independent runs.  
1136

Model	SI	SD	CD	SGD
LLMOB	0.1057 $\pm$ 0.0277	0.1509 $\pm$ 0.0386	0.0497 $\pm$ 0.0243	0.0319 $\pm$ 0.0170
LLM-MOB	0.1501 $\pm$ 0.0170	0.0558 $\pm$ 0.0208	0.0352 $\pm$ 0.0096	0.0532 $\pm$ 0.0430
LLM-MOVE	0.1242 $\pm$ 0.0035	0.0407 $\pm$ 0.0021	0.0131 $\pm$ 0.0007	0.0290 $\pm$ 0.0014
LLM-ZS	0.1601 $\pm$ 0.0071	0.1335 $\pm$ 0.0055	0.0155 $\pm$ 0.0008	0.0750 $\pm$ 0.0025
ELLMob	<b>0.0649<math>\pm</math>0.0030</b>	<b>0.0220<math>\pm</math>0.0044</b>	<b>0.0046<math>\pm</math>0.0012</b>	<b>0.0162<math>\pm</math>0.0018</b>

1144 Table A9: Stability analysis on the COVID-19 Pandemic dataset. Results are reported as Mean  $\pm$   
1145 Standard Deviation across 5 independent runs.  
1146

Model	SI	SD	CD	SGD
LLMOB	0.1128 $\pm$ 0.0173	0.1221 $\pm$ 0.0298	0.0158 $\pm$ 0.0038	0.0295 $\pm$ 0.0047
LLM-MOB	0.1099 $\pm$ 0.0107	0.0613 $\pm$ 0.0263	0.0191 $\pm$ 0.0072	0.0359 $\pm$ 0.0066
LLM-MOVE	0.1789 $\pm$ 0.0241	0.0511 $\pm$ 0.0044	0.0457 $\pm$ 0.0185	0.0544 $\pm$ 0.0067
LLM-ZS	0.1108 $\pm$ 0.0103	0.0551 $\pm$ 0.0025	0.0442 $\pm$ 0.0074	0.0605 $\pm$ 0.0056
ELLMob	<b>0.1002<math>\pm</math>0.0094</b>	<b>0.0443<math>\pm</math>0.0037</b>	<b>0.0079<math>\pm</math>0.0015</b>	<b>0.0279<math>\pm</math>0.0027</b>

1154 Table A10: Stability analysis on the Tokyo 2021 Olympics dataset. Results are reported as Mean  $\pm$   
1155 Standard Deviation across 5 independent runs.  
1156

Model	SI	SD	CD	SGD
LLMOB	0.1042 $\pm$ 0.0131	0.0291 $\pm$ 0.0036	0.0115 $\pm$ 0.0017	0.0054 $\pm$ 0.0006
LLM-MOB	0.1123 $\pm$ 0.0067	0.0338 $\pm$ 0.0083	0.0157 $\pm$ 0.0084	0.0172 $\pm$ 0.0127
LLM-MOVE	0.2027 $\pm$ 0.0050	0.0304 $\pm$ 0.0014	0.0111 $\pm$ 0.0009	0.0053 $\pm$ 0.0004
LLM-ZS	0.0953 $\pm$ 0.0021	0.0320 $\pm$ 0.0014	0.0147 $\pm$ 0.0021	0.0060 $\pm$ 0.0011
ELLMob	<b>0.0606<math>\pm</math>0.0016</b>	<b>0.0063<math>\pm</math>0.0002</b>	<b>0.0021<math>\pm</math>0.0002</b>	<b>0.0037<math>\pm</math>0.0002</b>

1165 **Initial trajectory generation.** Once the event context is established, this prompt generates an  
1166 initial trajectory. It takes the user’s long-term and short-term trajectories, and the structured event  
1167 context as input, instructing the model to synthesize this information into a plausible daily plan and  
1168 provide an analytical justification for its reasoning.1169 To facilitate the reflection module, the framework extracts three distinct forms of gist: Event Gist,  
1170 Action Gist, and Pattern Gist.1172 **Event Gist Generation.** This prompt distills the core behavioral takeaway for the public from the  
1173 event information.1175 **Action Gist Generation.** This prompt infers the underlying intent from the generated trajectory  
1176 and its accompanying justification.1178 **Pattern Gist Generation.** This prompt analyzes the user’s long-term and short-term trajectory  
1179 logs to synthesize their core behavioral patterns, including strengths (points of inertia) and weak-  
1180 nesses (points of fracture).1182 **Conflict Judgment.** This prompt serves as the core of the auditing mechanism. It instructs the  
1183 model to act as a Critical Trajectory Auditor to evaluate the coherence between the Action Gist, the  
1184 user’s Pattern Gist, and the situational Event Gist.1186 **Trajectory Regeneration.** If the planned trajectory fails the conflict audit, this prompt is invoked.  
1187 It instructs the model to act as a Trajectory Plan Corrector, using the auditor’s feedback to regenerate  
1188 a revised plan that specifically resolves all identified inconsistencies.

1188  
 1189 **Event context generation**  
 1190 # SYSTEM ROLE  
 1191 You are an expert event impact analyst. Your primary mission is to dissect the provided unstructured event text  
 1192 and transform it into a clear, actionable intelligence brief.  
 1193  
 1194 The data are as follows:  
 1195 <EVENT TEXT>: !<INPUT 0>!  
 1196  
 1197 # OUTPUT  
 1198 1. Event Profile:  
 1199 Extract the type, name, time, and location of the event.  
 1200 2. Intensity & Scale:  
 1201 Detail the key metrics of the event's power and its direct physical consequences (e.g., rainfall, storm surge).  
 1202 3. Infrastructure & Service Impact:  
 1203 List the critical infrastructure failures (e.g., power outages) and public service shutdowns (e.g., transportation, attractions).  
 1204 4. Official Directives:  
 1205 State the official orders and advisories issued, including the scale of the population they targeted.  
 1206  
 1207

Figure A6: The details of event schema under three different events.

1208  
 1209 **Initial trajectory generation**  
 1210 # SYSTEM ROLE  
 1211 Your task is to generate a user's trajectory based on activity patterns.  
 1212  
 1213 You will be provided with:  
 1214 - <LONG-TERM>: The user's historical stays showing their personal patterns.  
 1215 - <SHORT-TERM>: Recent contextual information about the user's activities.  
 1216 - <EVENT>: Current day event information (holidays, emergencies, or normal operations)  
 1217 - <DAY\_TYPE>: Indicates whether the current day is a weekday or a weekend  
 1218  
 1219 # CONTEXT & GOAL  
 1220 Please generate the trajectory considering:  
 1221 1. Event Impact Assessment: Check <EVENT> first to understand the day's context:  
 1222 - Event: First, check the <EVENT> and it establishes the main context for the day. It should be treated as the  
 1223 reference for today's trajectory generation.  
 1224 - During Holidays/Weekends: Expect an increase in leisure, social, and shopping activities. During Normal  
 1225 Weekdays: Assume regular routines.  
 1226  
 1227 2. Personal Patterns Priority: The user's individual patterns from <LONG-TERM> are the guide. Look for:  
 1228 - Regular visits to specific places at certain times.  
 1229 - Sequential activity patterns (places that frequently follow other places).  
 1230  
 1231 3. Recent-Aware Adaptation: Recent activities in <SHORT-TERM> may override personal if they indicate a  
 1232 change in routine.  
 1233  
 1234 4. Temporal Consistency: Ensure all timestamps are chronologically ordered and realistic for travel times  
 1235 between locations.  
 1236  
 1237 5. Analytical Justification (For the "reason" field): It must be a third-person, analytical summary explaining how  
 1238 you used the inputs to generate the plan. It should state the core pattern identified and mention the influence of  
 1239 the event.  
 1240  
 1241 The data are as follows:  
 1242 <LONG-TERM>: !<INPUT 0>!  
 1243 <SHORT-TERM>: !<INPUT 1>!  
 1244 <EVENT>: !<INPUT 2>!  
 1245 <DAY\_TYPE> !<INPUT 3>!  
 1246  
 1247 # OUTPUT  
 1248 Response STRICTLY to the prompt above in JSON in the \*following\* format:  
 1249 {"plan": [<Location> at <Time>, <Location> at <Time>, ...], "reason": ...}  
 1250  
 1251

Figure A7: The prompt of initial trajectory generation.

1242

1243

1244

1245

1246

1247

1248

1249

1250

1251

1252

1253

1254

1255

1256

1257

1258

1259

1260

1261

1262

1263

1264

1265

1266

1267

1268

1269

1270

1271

1272

1273

1274

1275

1276

1277

1278

1279

1280

1281

1282

1283

1284

1285

1286

1287

1288

1289

1290

1291

1292

1293

1294

1295

### Event gist generation

#### # SYSTEM ROLE

You are an expert event impact analyst.

Your analysis must go beyond surface-level facts to unearth the subtle cues that predict and explain public behavior in an event.

#### # INSTRUCTION

Analyze the [EVENT TEXT] provided below. Extract the following key information from the provided inputs to synthesize the event gist:

##### 1. Core Implication:

The simplified understanding of what this event means for mobility decisions.

##### 2. Behavioral Implications:

Survival, information gathering, social dynamics, and compliance

##### 3. Risk-Reward Calculus:

Returns on responding to event risks.

The data are as follows:

<EVENT TEXT>: !<INPUT 0>

#### # OUTPUT

##### \*\*Event Gist:\*\*

Directly state the \*\*gist\*\* that the public likely formed from the event information.

"Gist" can show how behaviors related to survival, information gathering, social dynamics, and risk-reward are all logical consequences of the public operating on this core interpretation.

Figure A8: The prompt of event gist generation.

### Action gist generation

#### # SYSTEM ROLE

You are a Decision Rationale Analyst. You specialize in deconstructing a planned action and its justification to assess its core intent.

You will be provided with:

- <PLANNED\_TRAJECTORY>: A candidate trajectory, defined as a specific sequence of planned locations and actions.
- <PLANNED\_TRAJECTORY\_REASON>: The justification and logic explaining the purpose behind the planned trajectory.

#### # INSTRUCTION

Analyze the <PLANNED\_TRAJECTORY> and <PLANNED\_TRAJECTORY\_REASON> to explicitly state the user's inferred "Action Gist" by considering following key information:

##### 1. Primary Intent:

The main purpose driving this trajectory choice.

##### 2. Habit Adherence:

Preservation versus compromise of habitual patterns.

##### 3. Event Compliance:

Adherence to event-imposed constraints.

The data are as follows:

- <PLANNED\_TRAJECTORY>: !<INPUT 0>!
- <PLANNED\_TRAJECTORY\_REASON>: !<INPUT 1>!

#### # OUTPUT

##### \*\*Action Gist:\*\*

Directly state the \*\*gist\*\* that summarizes the core intent of the planned trajectory.

Figure A9: The prompt of action gist generation.

1296  
 1297  
 1298  
 1299  
 1300  
 1301  
 1302  
 1303  
 1304  
 1305  
 1306 **Pattern gist generation**  
 1307 **# SYSTEM ROLE**  
 1308 You are an expert Behavioral Pattern Analyst. Your expertise is in synthesizing detailed activity logs into a high-  
 1309 level understanding of a person's life structure, identifying both its core strengths and critical dependencies.  
 1310 Your mission is to analyze an individual's long-term and short-term activity data to derive their "Pattern Gist".  
 1311 You need to consider the routine's core points of inertia (strengths) and points of fracture (weaknesses).  
 1312 You will be provided with:  
 1313 - <LONG-TERM>: The user's historical stays showing their personal patterns.  
 1314 - <SHORT-TERM>: Recent contextual information about the user's activities.  
 1315 **# INSTRUCTION**  
 1316 1. Synthesize the Core Behavior: Based on the [SHORT-TERM] and considering the [SHORT-TERM],  
 1317 first synthesize and clearly state the initial Pattern Gist. This should be a high-level summary of their dominant  
 pattern of action.  
 1318 Critical guidance: Your analysis must go beyond simply listing the most frequent, generic locations.  
 1319 The goal is to find the underlying purpose or narrative that connects these individual data points.  
 1320 Focus on what makes this person's pattern specific and characteristic.  
 1321 For example, is the combination of regular visits to a Government Office, an Elementary School, and a large  
 1322 Supermarket indicative of a "structured public servant's life",  
 1323 "a parent's daily routine" or "a mix of professional and family responsibilities"?  
 1324 Your gist must capture this deeper meaning and consider points of inertia and fracture.  
 1325 2. Identify Points of Inertia (Strengths):  
 1326 Based on the Pattern Gist, what are the most deeply embedded, almost non-negotiable components of the  
 1327 routine?  
 1328 Identify the rituals, obligations, or habits that create the strongest "pull" to maintain this pattern.  
 1329 3. Identify Points of Fracture (Weaknesses):  
 1330 What are the external dependencies required for the Pattern Gist to function?  
 1331 Identify the single points of failure (e.g., reliance on public transport, specific store availability, power grid) that,  
 if disrupted, would make this pattern impossible to follow.  
 1332 The data are as follows:  
 1333 <LONG-TERM>: !<INPUT 0>!  
 1334 <SHORT-TERM>: !<INPUT 1>!  
 1335 **# OUTPUT**  
 1336 **\*\*Pattern-Gist:\*\***  
 1337 Directly state the **\*\*gist\*\*** that embodies the core structure of the user's routine.  
 1338  
 1339

Figure A10: The prompt of pattern gist generation.

1340  
 1341  
 1342  
 1343  
 1344  
 1345  
 1346  
 1347  
 1348  
 1349

1350  
 1351  
 1352  
 1353  
 1354  
 1355  
 1356  
 1357  
 1358  
 1359  
 1360 **Conflict judgement**  
 1361 **# SYSTEM ROLE**  
 1362 You are a critical Trajectory Auditor. Your task is to perform a strict, logical audit to decide if a planned trajectory  
 1363 is aligned based on user's habitual mobility pattern and the current event context.  
 1364 You will be provided with:  
 1365 - <EVENT\_GIST>: Reflects the core impact, restrictions, and incentives of an external event on trajectory  
 1366 decisions.  
 1367 - <PATTERN\_GIST>: Distills the user's long-term, habitual mobility patterns.  
 1368 - <ACTION\_GIST>: Represents the intention of current mobility.  
 1369 **#CORE JUDGMENT**  
 1370 Your judgments must not be based on a **\*\*superficial or literal matching of words\*\***.  
 1371 Instead, you must evaluate if the inferred "Action Gist" represents a rational and mature decision for this  
 1372 specific pattern within the specific context of the event.  
 1373 1. Does the Action Gist conflict with the Pattern Gist?  
 1374 - Evaluate whether the action fundamentally contradicts the core pattern and whether it is a contextually  
 1375 appropriate adaptation.  
 1376 - Pattern Gist reflects general tendencies, not rigid rules. Use commonsense reasoning to decide whether the  
 1377 action still aligns with the character's core motivations, even if the surface behavior differs.  
 1378 - Do not consider temporary, situationally driven behaviors as a conflict if they are **\*\*clearly justified by the**  
 1379 **context\*\***.  
 1380 2. Does the Action Gist conflict with the Event Gist?  
 1381 - Evaluate whether the plan appropriately respond to the event's constraints.  
 1382 - Risk assessment should be comprehensive, not just venue-based.  
 1383 - Consider both immediate safety and contingency planning.  
 1384 The data are as follows:  
 1385 - <EVENT\_GIST>: !<INPUT 0>!  
 1386 - <PATTERN\_GIST>: !<INPUT 1>!  
 1387 - <ACTION\_GIST>: !<INPUT 2>!  
 1388 Your output MUST be in strict JSON format.  
 1389 **# OUTPUT**  
 1390 Your output MUST be in a strict JSON format with the following three keys:  
 1391 "coherence\_with\_pattern": A boolean value (true or false).  
 1392 "coherence\_with\_event": A boolean value (true or false).  
 1393 "reason": A detailed justification for the two judgments above with weakness if necessary.  
 1394  
 1395  
 1396  
 1397  
 1398  
 1399  
 1400  
 1401  
 1402  
 1403

Figure A11: The prompt of conflict judgment.

```

1404
1405
1406
1407
1408
1409
1410
1411
1412
1413
1414 Trajectory regeneration
1415 # SYSTEM ROLE
1416 You are a "Trajectory Plan Corrector". Your sole purpose is to fix a flawed plan based on an expert's audit
1417 report.
1418 # CONTEXT & GOAL
1419 A user's initial plan <LAST_PLAN> was evaluated by a Rationality Auditor and deemed irrational. The
1420 auditor's report <FAILED_PLAN_REASON> explains what was wrong. Your task is to generate a new, revised
1421 plan that **specifically addresses and resolves every concern** raised in the auditor's report. The auditor's
1422 feedback should be followed.
1423 You will be provided with:
1424 - <LONG-TERM>: The user's historical stays showing their personal patterns.
1425 - <SHORT-TERM>: Recent contextual information about the user's activities.
1426 - <EVENT>: Current day event information (holidays, emergencies, or normal operations)
1427 - <DAY_TYPE>: Indicates whether the current day is a weekday or a weekend
1428 - <LAST_PLAN>: The previous plan JSON that failed checking
1429 - <FAILED_LAST_PLAN_REASON>: The auditor's failure report
1430 # MANDATORY CORRECTION PROCESS
1431 1. EXTRACT every failure point from <FAILED_PLAN_REASON>
1432 2. MAP each failure to a specific correction
1433 3. VERIFY no failure point is missed
1434 4. VALIDATE the new plan against ALL criteria
1435 The new "plan" should be the corrected trajectory.
1436 Temporal Consistency: Ensure all timestamps are chronologically ordered and realistic for travel times
1437 between locations. The "reason" should be an overall justification for the new plan. Analytical Justification (For
1438 the "reason" field): It must be a third-person, analytical summary explaining how you used the inputs to
1439 generate the plan. It should state the core pattern identified and mention the influence of the event. Generate
1440 your response as a single JSON object.
1441
1442 The data are as follows:
1443 <LONG-TERM>: !<INPUT 0>!
1444 <SHORT-TERM>: !<INPUT 1>!
1445 <EVENT>: !<INPUT 2>!
1446 <DAY_TYPE>: !<INPUT 3>!
1447 <LAST_PLAN>: !<INPUT 4>!
1448 <FAILED_LAST_PLAN_REASON> !<INPUT 5>
1449 # OUTPUT
1450 Response STRICTLY to the prompt above in JSON in the *following* format:
1451 {"plan": [<Location> at <Time>, <Location> at <Time>,...], "reason":...}
1452
1453
1454
1455
1456
1457

```

Figure A12: The prompt of trajectory regeneration.